AAC
Journals.ASM.org

Disuccinyl Betulin Triggers Metacaspase-Dependent Endonuclease G-Mediated Cell Death in Unicellular Protozoan Parasite *Leishmania donovani*

Sayan Chowdhury,[a] Tulika Mukherjee,[b] Somenath Roy Chowdhury,[a] Souvik Sengupta,[c] Sibabrata Mukhopadhyay,[b] Parasuraman Jaisankar,[b] Hemanta K. Majumder[a]

Molecular Parasitology Laboratory, Indian Institute of Chemical Biology, Kolkata, India[a]; Department of Chemistry, Indian Institute of Chemical Biology, Kolkata, India[b]; Laboratory of Molecular Biology, Department of Physical Chemistry, Indian Association for the Cultivation of Sciences, Kolkata, India[c]

The unicellular organism *Leishmania* undergoes apoptosis-like cell death in response to external stress or exposure to antileishmanial agents. Here, we showed that 3-*O*,28-*O*-disuccinyl betulin (DiSB), a potent topoisomerase type IB inhibitor, induced parasitic cell death by generating oxidative stress. The characteristic feature of the death process resembled the programmed cell death (PCD) seen in higher eukaryotes. In the current study, the generation of reactive oxygen species (ROS), followed by the depolarization of mitochondrial membrane potential ($\Delta\Psi_m$), caused a loss in ATP production in *Leishmania* parasites. This further gave positive feedback to produce a large amount of ROS, which in turn caused oxidative DNA lesions and genomic DNA fragmentation. The treatment of promastigotes with DiSB induced high expression levels of metacaspase protein that led to cell death in this unicellular organism. The PCD was insensitive to benzyloxycarbonyl-Val-Ala-Asp(OMe)-fluoromethylketone (zVAD-fmk), suggesting that the death process was not associated with the activation of caspases. DiSB treatment translocated *Leishmania donovani* endonuclease G (LdEndoG) from mitochondria to the nucleus, which was responsible for the DNA degradation process. Conditional antisense knockdown of *L. donovani* metacaspase (LdMC), as well as EndoG, -subverted death of the parasite and rescued cell cycle arrest in G_1 phase. The present study on the effector molecules associated with the PCD pathway of the parasite should help to manifest the mechanisms of PCD and also might be exploited in antileishmanial chemotherapy.

Cell death, particularly apoptosis, is one of the most widely studied phenomena by cell biologists. Understanding apoptosis under disease conditions is very important, as it not only gives insights into the pathogenesis of a disease but also leaves clues on how the disease can be treated. Type I programmed cell death (PCD) involves three main types of biochemical changes, (i) the activation of caspases, (ii) DNA and protein breakdown, and (iii) membrane changes and recognition by phagocytic cells (1). Early in apoptosis, phosphatidylserine (PS) is expressed in the outer layers of the cell membrane, which has been "flipped out" from the inner layers. This allows early recognition of the dead cells by macrophages, resulting in phagocytosis without the release of proinflammatory cellular components (2). In higher eukaryotes, activated caspase-3 activates caspase-activated DNases (CADs) (3). Endonuclease G (EndoG) (4) and apoptosis-inducing factor (AIF) comprise caspase-independent effector endonucleases. Cytotoxic agents induce oxidative stress and cause the nuclear translocation of EndoG, which thereby induces DNA fragmentation and PCD (5).

Leishmaniasis is the most serious form of parasitic diseases caused by the protozoan flagellates of the genus *Leishmania*, and it has a spectrum of clinical presentations (6). More than 350 million people are at risk for the infection, and the disease causes 70,000 deaths each year (7). The control measures that are mainly based on early detection and chemotherapy are hampered by huge toxicity, side effects of the drugs, and the emergence of drug-resistant parasites. For the last 6 decades, organic pentavalent antimonials (Sb^V) have been the first-line drugs for treatment of this disease. However, the emergence of isolates that are clinically resistant to these drugs poses a serious obstacle for disease control and treatment (8). Therefore, the need to identify new molecular targets for improved therapy is clear and justified. A better understanding of the cell death mechanism induced by drugs will be helpful in developing intervention strategies against the parasites.

In *Leishmania* spp., PCD helps in altruistic growth control and organizes them into clonal populations (9) by (i) selecting for the fitter cells within the population, (ii) optimally regulating the cell number to adapt to the environmental constraints, and (iii) tightly controlling the cell cycle and cell differentiation. Topoisomerases are DNA manipulators that relieve the torsional strain in DNA that is built up during vital cellular processes. The heterodimeric topoisomerase IB of *Leishmania* has been established as an attractive therapeutic target (10). In higher eukaryotes, so-called DNA sensors recognize inhibitor trapped topoI-DNA cleavable complex and activate Bax to subtly permeabilize the mitochondrial outer membrane. This generates oxidative stress and causes nascent cytochrome *c* release (11). Cytochrome *c* forms the "apoptosome," binds to inositol triphosphate receptors, and releases Ca^{2+} into the cytosol (12). The maintenance of the proper mitochondrial transmembrane potential ($\Delta\psi_m$) is essential for survival of the cell because it drives the synthesis of ATP and main-

Received 9 October 2013 **Returned for modification** 6 December 2013
Accepted 23 January 2014
Published ahead of print 27 January 2014
Address correspondence to Hemanta K. Majumder, hkmajumder@iicb.res.in.

doi:10.1128/AAC.02193-13

tains oxidative phosphorylation (13). In caspase-independent PCD, the increase in intracellular calcium increases mitochondrial calcium and causes further mitochondrial membrane depolarization, the generation of reactive oxygen species (ROS), and the activation of endonucleases (3). In *Leishmania*, the potent topoisomerase IB inhibitor camptothecin (CPT) is known to induce DNA degradation and PCD (14).

Betulin [lup-20(29)-ene-3β,28-diol], an abundant and naturally occurring triterpene, and its derivative betulinic acid, exhibit antimalarial (15), anti-HIV, and anti-inflammatory (16) properties, as well as cytotoxic activities on cancer cell lines (17). Betulin derivatives are chemically synthesized products, which affect DNA-topoisomerase activity (18). Betulin induces apoptotic cell death and inhibits the growth of human gynecologic and colon cancer cells (19). Treatment with betulin also alters the morphology of tumor cells, decreasing their motility and inducing apoptotic cell death. Betulin induces cell death more rapidly than does betulinic acid, but to achieve a similar degree of cell death, a considerably higher concentration of betulin is needed (20). Although a few reports exist that show antiprotozoal activities of betulin derivatives, there is no extensive study on cell death induced by betulin derivatives (21, 22, 23). We have shown that 3-*O*,28-*O*-disuccinyl betulin (DiSB) is a potent antileishmanial agent that binds to topoisomerase I and inhibits the binding of the enzyme to DNA, which thus affects the relaxation activity of *Leishmania* topoisomerase (18). DiSB is also effective at reducing the parasite burden in cultured macrophages and is effective against sodium antimony gluconate (SAG)-resistant parasites (18).

In the present study, we have shown that DiSB induces caspase-independent PCD of the parasites. While studying nuclear, mitochondrial, and cytosolic changes associated with PCD, it was found that the compound causes depolarization of the mitochondrial membrane. The loss of $\Delta\psi_m$ leads to the release of cytochrome *c* into the cytosol, and cell death is then triggered by the activation of metacaspases. This is evidenced by downregulation of the DiSB-mediated cell death process after the inhibition of metacaspase activity. Taken together, our results provide an insight into the mitochondrion-dependent apoptotic-like death pathway induced by DiSB in *Leishmania* spp. Depletion of the ATP level enhances apoptosis by creating cellular oxidative stress, followed by DNA fragmentation, which is caused by nuclear translocated mitochondrial LdEndoG. Such information has great potential in determining the role of mitochondria in the apoptosis-like death of leishmanial cells and in designing better drugs for leishmaniasis.

MATERIALS AND METHODS

Chemicals. DiSB, 3-*O*,28-*O*-diglutaryl dihydrobetulin (DiGDHB), 3-*O*,28-*O*-disuccinyl dihydrobetulin (DiSDHB) (18), CPT, *N*-acetyl cysteine (NAC) (20 mM concentration each), carbonyl cyanide *m*-chlorophenyl hydrazone (CCCP) (100 mM), 1,2-bis(*o*-aminophenoxy)ethane-N,N,N′,N′-tetraacetic acid (BAPTA-AM) (50 mM), and H_2DCFDA (10 mM) were dissolved in 100% dimethyl sulfoxide (DMSO) and stored at −20°C. Antipain (10 mM) and aurintricarboxylic acid (ATA) (ammonium salt at 20 mM) were dissolved in water and stored at −20°C. All the above chemicals were purchased from Sigma-Aldrich (St. Louis, MO, USA). *cis*-Parinaric acid was purchased from Life Technologies (Carlsbad, CA, USA).

Parasite culture and maintenance. *Leishmania donovani* (strain MHOM/IN/AG/83) promastigotes were grown at 22°C in M199 medium supplemented with 10% fetal calf serum, as described previously (24). For knockdown studies, the *Leishmania tarentolae* T7.TR strain (Jena Bioscience) was used (25). To maintain the genome-integrated T7 RNA polymerase and Tet repressor genes, the parasites were cultured in the presence of nourseothricin and hygromycin (100 μg/ml each).

Measurement of cell viability. The *L. donovani* AG83 promastigotes were treated with different concentrations (1, 2.5, 5, 10, or 25 μM) of DiSB, DiGDHB, and DiSDGB for 12 h. In another set of experiment, promastigotes (3.0×10^6 cells/ml) were incubated with three different concentrations of DiSB (1, 5, or 10 μM) for the indicated time periods (2, 4, 6, 8, 10, 12, 16, or 24 h). The viability of promastigotes was measured using AlamarBlue dye. The dye is a cell permeable nontoxic nonfluorescent active ingredient (blue) that uses the natural reducing power of viable cells to convert resazurin to the fluorescent molecule, resorufin (very bright red). Metabolically active cells convert resazurin to resorufin, thereby generating a quantitative measure of viability and cytotoxicity (10).

Measurement of oxygen consumption. *L. donovani* AG/83 promastigotes (5×10^6 cells/ml) were grown in M199 medium containing 5 and 10 μM DiSB or 0.2% DMSO. Aliquots of cells were taken at indicated time intervals, harvested, and washed with respiration buffer (50 μM sucrose, 145 μM KCl, 5 μM NaCl, 1 μM EDTA, 1 μM $MgCl_2$, and 10 μM sodium phosphate buffer [pH 7.4]) and finally suspended in the same buffer. Oxygen uptake was determined with a Clarke-type oxy-electrode with a cell capacity of 2 ml (14). Calibration of the oxy-electrode was carried out using air-saturated water containing sodium metabisulfite.

Measurement of ROS. Intracellular ROS levels were measured in DiSB-treated and untreated parasites. Promastigotes (2×10^7 cells/ml) were treated with 5 or 10 μM DiSB for the indicated times. Parasites treated with 0.2% DMSO served as controls. In another set, the parasites were incubated with *N*-acetyl cysteine (NAC) prior to treatment with DiSB. The parasites were washed and resuspended in 500 μl of M199 (without phenol red) and incubated with a cell-permeant dye, H_2DCFDA, for 30 min (25). Fluorometric measurements (λ_{ex} = 510 nm and λ_{em} = 525 nm) were performed in triplicate, and the results were expressed as the mean fluorescence intensity per 10^6 cells.

Measurement of GSH and GSSG levels. The reduced glutathione (GSH) level was measured by a monochlorobimane dye that gives a blue fluorescence when bound to glutathione (14). *L. donovani* promastigotes (approximately 3×10^6 cells) were treated with or without DiSB for different times. The cells were then harvested and lysed by cell lysis buffer according to the manufacturer's protocol (ApoAlert glutathione assay kit; Clontech, Mountain View, CA). The cell lysates were incubated with monochlorobimane (2 μM) for 3 h at 37°C. The decrease in glutathione levels in the extracts of nonapoptotic and apoptotic cells was detected by a fluorometer with 395 nm excitation and 480 nm emission wavelengths and normalized to the total cell numbers. The spectrofluorometric data presented here are representative of three experiments.

For reduced glutathione detection, the glutathione fluorometric assay kit (measuring GSH, oxidized glutathione [GSSG], and total glutathione) from BioVision (catalog no. K264-100) was used. The preparation was done according to the manufacturer's protocol. Briefly, 2×10^6 cells were treated with DiSB (5 or 10 μM) for 8 h or after pretreatment with NAC. The cells were lysed in 100 μl of glutathione assay buffer. Sixty microliters of each lysate was transferred to a prechilled tube containing perchloric acid (PCA) and vortexed for several seconds to achieve uniform emulsion. Finally, the emulsions were kept on ice for 5 min and centrifuged for 2 min at 13,000 × *g* and 4°C, and the supernatant (containing glutathione) was collected. Total GSH and GSSG were measured according to the manufacturer's protocol.

Measurement of total fluorescent lipid peroxidation product. DiSB-treated and untreated *L. donovani* cells were centrifuged and pellets were washed twice with 1× phosphate-buffered saline (PBS). The pellets were suspended in 500 μl of 1× PBS. The cell suspension was further incubated with *cis*-parinaric acid (final concentration, 5 μM) and incubated in the dark at room temperature for 30 min (26). The fluorescence intensities of

the total fluorescent lipid peroxidation products were measured, with excitation at 320 nm and emission at 415 nm and expressed as relative fluorescence units. The spectrofluorometric data (normalized with total number of promastigotes) presented here are representative of three experiments.

Double staining with annexin V and PI. Externalization of phosphatidylserine on the outer membrane of untreated and DiSB-treated promastigotes was measured by binding fluorescein isothiocyanate (FITC)-annexin V and propidium iodide (PI) using an annexin V staining kit (Invitrogen Corporation, Ltd.). Flow cytometry was carried out for treated and untreated parasites. The gating was done so that the FL-1 channel denotes the mean intensity of FITC-annexin V, whereas the FL-2 channel denotes the mean intensity of PI. The data represented here are from one of three experiments.

Intracellular Ca^{2+} measurement. Intracellular Ca^{2+} concentration was measured with the fluorescent probe fura-2-acetoxymethyl ester (fura-2 AM), as described previously (27). Briefly, cells from differently treated groups were harvested and washed twice with wash buffer containing 116 μM NaCl, 5.4 μM KCl, 0.8 μM $MgCl_2$, 5.5 μM glucose, 1 μM $CaCl_2$, and 50 μM morpholinepropanesulfonic acid (MOPS) (pH 7.4). The cells were then suspended in the same buffer containing 15% sucrose and were incubated with fura-2 AM (6 μM) at 27°C for 1 h with mild shaking. The cells were pelleted down, and after two subsequent washings, they were suspended in the same wash buffer. Fluorescence measurements were performed with excitation at 340 nm and emission at 510 nm. To convert fluorescent values into absolute calcium concentrations, calibration was performed at the end of the each experiment. Cytosolic Ca^{2+} concentration was calculated using the equation $[Ca^{2+}] = K_d(F - F_{min})/(F_{max} - F)$, where K_d is the dissociation constant of the calcium-bound fura 2 complex (224 nM), F_{max} corresponds to the maximum fluorescence obtained by treating cells with 10 μM calcium ionophore A23187, and F_{min} represents the minimum fluorescence of the cells (obtained from ionophore-treated cells in the presence of 4 μM EGTA). The data were normalized with mg of total cellular protein extracts.

Measurement of $\Delta\Psi_m$. Mitochondrial transmembrane potential was investigated using JC-1 dye. This dye accumulates in the mitochondrial matrix under the influence of $\Delta\Psi_m$, where it reversibly forms monomers (green) with characteristic absorption and emission spectra (14). In brief, leishmanial cells, after treatment with DiSB (5 or 10 μM), or with 10 μM DiSB after 60 min pretreatment with NAC (20 μM), BAPTA-AM (25 μM), zVAD-fmk (25 μM), *N*α-*p*-tosyl-L-lysine chloromethyl ketone (TLCK) (1 μM), or antipain (2 μM) were harvested and washed with PBS (1×). The cells were then incubated at 28°C in a 5% CO_2 incubator for 1 h, with a final concentration of JC-1 dye at 5 μg/μl. The cells were then analyzed by fluorescence measurement with a spectrofluorometer, using 507 and 530 nm as the excitation and emission wavelengths, respectively, for green fluorescence, and 507 and 590 nm as excitation and emission wavelengths, respectively, for red fluorescence, to analyze $\Delta\Psi_m$. The spectrofluorometric data presented here are representative of three experiments. The ratio of the reading at 590 nm to the reading at 530 nm (590:530 ratio) was considered to be the relative $\Delta\Psi_m$ value. In a flow cytometer, the FL-1 channel denotes the mean fluorescence intensity.

Measurement of cellular ATP level. ATP content was determined by the luciferin/luciferase method, as described previously (14). The assay is based on the requirement of luciferase for ATP in producing light (emission maximum, 560 nm, at pH 7.8). In brief, promastigotes (3×10^7) were treated with different concentrations of drugs for the indicated times, washed with PBS (1×) twice, and suspended in PBS (1×). The mitochondrial and cytosolic extracts were prepared as described above. An aliquot of these fractions was assayed for ATP using the luciferase ATP assay kit (Invitrogen, Inc., Ltd.). The amount of ATP in the experimental samples was calculated from a standard curve prepared with ATP. The data were normalized to mg of cellular protein extract.

Cell fractionation. The nuclear/kinetoplast (N/K) fraction was prepared by lysing parasites with 140 μM NaCl, 1.5 μM $MgCl_2$, 10 μM Tris-HCl (pH 8.6), 0.5% NP-40, and protease inhibitors. After 10 min, the cell suspension was centrifuged at 6,000 × *g* for 5 min at 4°C. The supernatant served as the cytosolic fraction, whereas the pellet was the N/K fraction (as both share a more or less similar mass for kinetoplastids). For immunoblotting analysis, the nuclear extract was prepared by resuspending the N/K fraction in the same buffer with 0.25 mg/ml digitonin and 100 U of DNase I. The suspension was kept for 15 min at room temperature. Thereafter, it was centrifuged at 10,000 × *g* for 10 min at 4°C. The supernatant served as the nuclear extract. The mitochondrial pellet was resuspended in the same buffer containing 1 mg/ml digitonin and 0.5% Triton X-100. After incubation for 10 min at room temperature, the suspension was centrifuged at 12,000 × *g* for 10 min at 4°C to obtain the mitochondrial fraction.

Preparation of cytoplasmic extract. Cytoplasmic extracts were prepared from both treated and untreated *Leishmania* cells, as described previously (14). In brief, cells (3×10^7) after different treatments were harvested, suspended in cell extraction buffer (20 μM HEPES-KOH, 10 μM KCl, 1.5 μM $MgCl_2$, 1 μM EDTA, 1 μM dithiothreitol, 200 μM phenylmethylsulfonyl fluoride (PMSF), and 10 μg/ml leupeptin and pepstatin), and lysed by a freeze-thaw process using nitrogen cavitations and incubating at 37°C for 5 min simultaneously. The lysate was centrifuged at 10,000 × *g* for 1 h, and the supernatants were used as a source of cytoplasmic extract.

Detection of cytochrome *c* release by Western blotting. DiSB-treated and untreated cells were harvested and washed twice with 1× PBS, suspended in cell fractionation buffer (ApoAlert cell fractionation kit), and homogenized. After separation of the cytosolic and mitochondrial fractions, 50 μg of each of the cytosolic fractions was separated by electrophoresis on 12% SDS-polyacrylamide gel and immunoblotted with the rabbit polyclonal cytochrome *c* antibody. Horseradish peroxidase-conjugated secondary antibody was used, and the protein band was visualized by enhanced chemiluminescence reaction.

Metacaspase activity. The fluorogenic substrates Boc-GRR-AMC were obtained from Bachem (Bubendorf, Switzerland), and Ac-DEVD-AMC, Ac-VEID-AMC, and Ac-LEHD-AFC were from Molecular Probes. The caspase inhibitor zVAD-fmk was obtained from Calbiochem. All the other protease inhibitors were obtained from Sigma (St. Louis, MO). *L. donovani* promastigotes (5×10^6) were treated with DiSB or without for different time periods. Different group of cells were pretreated for 60 min with NAC, antipain, TLCK, or zVAD-fmk, followed by DiSB treatment. The cells were then harvested and lysed by cell lysis buffer according to the manufacturer's protocol (ApoAlert caspase assay kit; Clontech). The cell lysates were incubated with respective caspase or metacaspase buffers to detect CED3/CPP32 and interleukin-converting enzyme (ICE) group of protease or metacaspase activities. Individual fluorogenic peptide substrates at 100 μM and 1× reaction buffer containing 100 μM dithiothreitol (DTT) were added to the corresponding cell lysates. 7-Amino-4-trifluoromethylcoumarin (AFC) and 7-amino-4-methylcoumarin (AMC) release were measured after incubating these samples at 37°C for 2 h by a fluorometer, with 400 nm excitation and 500 nm emissions and 380 nm excitation and 460 nm emissions, respectively. The data were normalized with mg of total cellular protein extracts.

Generation of antisense constructs. Antisense constructs of LdMC were generated by PCR amplification of the 1 to 177 nucleotide region using sense primer 5′-CGGGATCCATGATCGCCCGGCTGCTCGGC-3′ and antisense primer 5′-CCCAAGCTTTCACTGGCTGCTGCTGTCGCT-3′ and cloned in the antisense orientation in the HindIII/BamHI site of pLew82v4. It was electroporated into Lt.T7.TR strain (Jena Bioscience), and transfectants were selected using phleomycin and termed antiMC. For control, empty vector transfectant was also prepared and termed pLew82. Tetracycline (2 μg/ml) induction for 24 h was carried out in both the transfectants, after which DiSB treatment was done.

Parasite growth in LdEndoG- and LdMC-downregulated parasites. Wild-type LdEndoG and LdMC were downregulated separately using the conditional antisense approach described previously (25). DiSB treat-

ment was carried out after 24 h of tetracycline induction in the abovementioned transfectants, whereas the pLew82 transfectants served as the empty vector control. Live promastigotes were calculated at given time intervals. Three sets of experiments were carried out, and the values were averaged and plotted.

DNA fragmentation assay. An estimate of the extent of DNA fragmentation after drug treatments was carried out using the cell death detection enzyme-linked immunosorbent assay (ELISA) kit (Roche Biochemicals). Promastigote samples (5×10^6 cells/ml) were collected at different time intervals, and the histone-associated DNA fragments (mononucleosome and oligonucleosome) were detected using the manufacturer's protocol. DNA fragmentation was estimated by spectrophotometric measurement of microtiter plates in a Thermo Multiskan EX plate reader at 405 nm. The results were normalized with the number of total parasites. The relative percentages (with respect to samples treated with micrococcal nuclease and normalized to percentage values) were plotted versus time.

Genomic DNAs from exponentially growing *L. donovani* promastigotes (2×10^6) treated with DiSB or without and H_2O_2 were isolated with an apoptotic DNA ladder kit (Roche Biochemicals). In another set, *L. donovani* promastigotes were separately preincubated with 2 μM antipain for 1 h, followed by treatment with 10 μM DiSB for different time points. DNAs were electrophoresed in 1% agarose gel at 75 V for 2 h, stained with ethidium bromide, and photographed under UV illumination.

***In situ* labeling of DNA fragments by terminal deoxyribonucleotidyl transferase (TdT)-mediated dUTP nick-end labeling.** Treated and untreated *L. donovani* promastigote cells were fixed with 2% paraformaldehyde and incubated with 0.5% Triton X-100 for 5 min for permeabilization and layered with a TdT reaction mixture containing FITC-labeled dUTP for 1 h at 37°C, according to the manufacturer's protocol (ApoAlert DNA fragmentation assay kit). The cells were stained with propidium iodide and acquired by BD FACSAria II flow cytometer through dual pass FITC/PI filter set. The data were analyzed by BD FACScan software.

Assay of PARP cleavage. Cell lysates were prepared from DiSB-treated and untreated cells, separated on 12% SDS-polyacrylamide gel, and subjected to Western blot analysis as described previously (14). Anti-poly (ADP-ribose) polymerase (PARP) polyclonal antibody diluted to 1,000-fold and horseradish peroxidase-conjugated secondary antibody were used to visualize the reactive band by chemoluminescence reaction.

Cell cycle analysis. Exponentially grown *L. donovani* promastigote cells (2.5×10^6) were treated with DiSB (10 μM) for 2, 4, 6, or 8 h. The cells were then harvested, washed three times with PBS (1×), and fixed in 50% ethanol (diluted in 1× PBS) for 4 h. The fixed cells were washed thoroughly, treated with 100 μg/ml RNase A, and then suspended in 1 ml of staining solution (1 mg/ml stock solution of PI diluted to 3 μM PI in staining buffer [100 μM Tris {pH 7.4}, 150 μM NaCl, 1 μM $CaCl_2$, 0.5 μM $MgCl_2$, 0.1% Nonidet P-40]). The samples were incubated for 30 min in the dark at room temperature and were analyzed by flow cytometry. The cells (20,000) were analyzed from each sample. The percentage of cells in G_1, S, and G_2/M phases of the cell cycle were determined in a Becton, Dickinson flow cytometer, and the data were processed by BD FACScan Software (San Diego, CA).

***In vivo* analysis of BrdU incorporation.** Promastigotes were treated with DiSB for different time periods, and the samples were labeled with bromodeoxyuridine (BrdU) for 2 h, fixed with ethanol, and then incubated with a monoclonal antibody to BrdU. The antibody to BrdU supplied with the kit (Roche Biochemicals) contains an optimized mixture of nucleases. These nucleases generate single-stranded DNA fragments, which allow for binding of the antibody to BrdU without destruction of the cellular morphology. The samples were incubated in the presence of anti-BrdU antibody raised in mice. The samples were counterstained with propidium iodide (in the presence of 10 μg/ml RNase). The samples were acquired in BD FACSAria II and the data were analyzed using BD FACScan software.

Measurement of *in vivo* DNA synthesis. Exponentially growing *L. tarentolae* promastigote cells (8×10^6 cells/ml) were radiolabeled by adding [*methyl*-^{3}H]thymidine to final concentration of 5 μCi/ml (GE Healthcare, Chalfont St. Giles, Buckinghamshire, United Kingdom) into M199 medium supplemented with 10% heat-inactivated fetal bovine serum (FBS). The cultures were incubated for 4 to 24 h at 22°C in presence or absence of different concentrations of DiSB. After incubation, the cells were lysed with 10% trichloroacetic acid and harvested in a Skatron Combi cell harvester. The readings were normalized with the total number of parasites. The incorporation of radioactivity in acid-precipitable DNA was measured in a liquid scintillation counter, as described previously (10).

RESULTS

Betulin derivatives inhibit growth of *Leishmania* sp. promastigotes. *L. donovani* AG83 promastigotes (3.0×10^6 cells/ml) were incubated with different concentrations (1, 2.5, 5, 10, or 25 μM) of three different betulin derivatives (DiSB, DiGDHB, or DiSDHB) up to 12 h, after which the number of live promastigotes were estimated with AlamarBlue reagent (Fig. 1A). The 50% effective concentrations (EC_{50}s) were 1.43 ± 0.24, 1.51 ± 0.35, and 3.32 ± 0.81 μM for DiSB, DiGDHB, and DiSDHB, respectively. A previous study showed that these betulin derivatives are potent topoisomerase inhibitors and kill intracellular parasites (18). All three compounds are very effective against the *L. donovani* promastigotes and inhibit almost 90 to 98% of the growth of the parasite. DiSB shows about 98% inhibition of growth of the parasites in culture medium (Fig. 1A), so we performed our study thereafter with DiSB. At 12 h, 90% growth was inhibited by 1 μM DiSB, which was comparable to the inhibition (92%) achieved by 10 μM DiSB at 8 h, and 98% growth was inhibited by 5 μM DiSB at 16 h, which was comparable to the inhibition achieved by 10 μM DiSB at 12 h (Fig. 1B). Consistent with these results, it was observed that after 6 h treatment with 20 μM DiSB, the growth of *L. major*, *L. donovani*, and *L. tarentolae* promastigotes were inhibited to the extent of 90, 89, and 93%, respectively (Fig. 1C). The IC_{50}s for these leishmanial strains (after 6 h of culturing) were 7.21 ± 2.11, 5.84 ± 1.06, and 8.32 ± 2.03 μM for *L. donovani*, *L. major*, and *L. tarentolae*, respectively. We further extended our study with the growth inhibition of parasites resistant to sodium antimony gluconate (GE1), miltefosine (Mil), camptothecin (CPT), and diindolylmethane (DIM) (Fig. 1D). All the parasites showed a similar kind of growth inhibition in the presence of different concentrations of DiSB for 6 h, while untreated controls proliferated at a normal rate. Microscopic examination of all the samples indicated that the observed effect is leishmanicidal (as the promastigotes were lysed) rather than leishmanistatic. This was confirmed by microscopy. Therefore, our present data demonstrate that under *in vitro* conditions, DiSB can prove to be a highly cytotoxic leishmanicidal compound.

Treatment with DiSB hampers cellular oxygen consumption and causes induction of reactive oxygen species generation. Oxygen uptake was measured in the DiSB-treated and untreated (0.2% DMSO) parasites with time. *L. donovani* promastigotes consumed oxygen at the rate of 68 ± 14 nmol/min/mg of protein, remaining unchanged for 6 h. Treatment with 10 μM DiSB decreased the oxygen consumption rate to 31 ± 9 nmol/min/mg of protein in 2 h and to 12 ± 0.8 nmol/min/mg of protein in 6 h.

The cytotoxic activity of betulin on many cancer cells is attributed to its pro-oxidant activity through the generation of ROS (20). This prompted us to examine ROS production in *L. don-*

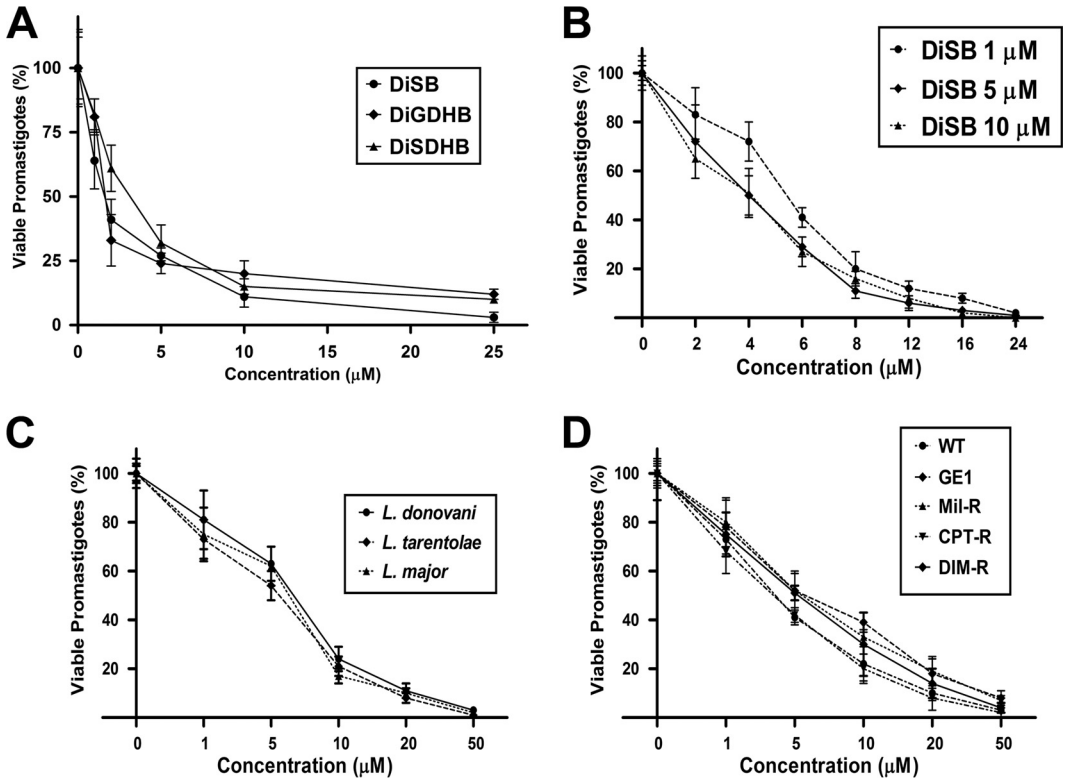

FIG 1 Betulin derivatives kill *Leishmania* parasites in a dose- and time-dependent manner. (A) Promastigotes were cultured in the presence of 0.2% DMSO or different concentrations of DiSB, DiGDHB, or DiSDHB up to 12 h. After 12 h, the percentages of viable promastigotes were calculated using AlamarBlue dye. The values were taken in triplicate and averaged. The percentages of live promastigotes were calculated and plotted against concentration. (B) Analysis of antileishmanial activity in the presence of 1 μM, 5 μM, or 10 μM DiSB for indicated times. The percentages of viable promastigotes were measured as described above. (C) *L. major*, *L. donovani*, and *L. tarentolae* promastigotes were also cultured in the presence of increasing concentrations of DiSB for 6 h. The percentages of viable promastigotes were measured by AlamarBlue assay. All data are expressed as a percentage of live promastigotes and represent the mean ± standard deviation (SD) values from three independent experiments. (D) Wild-type AG83 (WT), laboratory-grown sodium antimony gluconate-resistant cells (GE1), miltefosine-resistant *Leishmania* (Mil-R), camptothecin-resistant cells (CPT-R), and diindolylmethane-resistant strains (DIM-R) were cultured separately in FBS-supplemented M199 medium. Early log-phase promastigote cells (3×10^6) were treated with 1, 5, 10, 20, or 50 μM DiSB for 6 h. The percentages of live promastigotes were calculated as above and plotted. The data represent mean ± SD values ($n = 3$).

ovani promastigotes to determine if DiSB could trigger oxidative stress that might serve as a prerequisite for apoptosis-like cell death. During oxidative phosphorylation, the release of ROS in the form of superoxide anion occurs to the extent of 3 to 5% of the total oxygen consumed (28). However, under certain conditions in which drugs inhibit oxidative phosphorylation or cellular processes, this rate of ROS production can be increased greatly (29). To verify the effect of DiSB on intracellular ROS levels, we treated *Leishmania* parasites separately with DiSB (10 μM) and antioxidant (NAC) and examined the ROS production over time (Fig. 2B). Cellular ROS formation after treatment with DiSB in *L. donovani* promastigotes was measured fluorometrically by conversion of CM-H_2DCFDA to the highly fluorescent 2,7-dichlorofluorescein. The level of ROS increased in parasites significantly within 2 h of treatment with DiSB and increased up to 4 h of incubation. Treatment with DiSB generated a 3.7-fold larger amount of ROS (compared to DMSO treatment) inside the parasites. When cells were treated with NAC before treatment with DiSB (10 μM), the level of ROS generation decreased (Fig. 2B) to almost 2.3-fold at 4 h compared with DiSB at 10 μM treatment.

Oxidative stress causes depletion of GSH level and upregulation of lipid peroxidation. One of the most important cellular defenses against intracellular oxidative stress is GSH, which plays a critical role in mediating apoptosis in eukaryotes, including in leishmanial cells. The actual mechanism by which GSH exerts its influence in leishmanial cells is yet to be explored. GSH is an important molecule for protecting kinetoplastids from ROS or toxic compounds (27), and an increase in ROS may induce a loss of $\Delta\psi_m$. DiSB caused a 22% decrease in the GSH level after 2 h (Fig. 3A), and the effect was more pronounced after 4 h of treatment with DiSB (52%). When the cells were preincubated with NAC for 30 min, before treatment with DiSB, the decrease in GSH level was protected significantly, and the level tended to become normal. The generation of ROS in the parasites may have caused a concomitant decrease in the cellular trypanothione (GSH) levels (Fig. 3A). A decrease in the cellular GSH level produced oxidized GSSG levels inside cells. As a result, GSH to GSSG decreased in a time-dependent manner (Fig. 3B). When cells were pretreated with ROS scavenger NAC, GSH levels reverted back to the level of untreated controls.

Lipid peroxidation was assessed by measuring the total fluorescent lipid peroxidation products in leishmanial cells after treatment with DiSB. The treatment led to an increase (almost 2.6-fold) in lipid peroxides after 2.5 h and reached a saturating level (4.5-fold) after 5 h. When leishmanial cells were treated with butylated hydroxytoluene (BHT) (20 μM), a specific in-

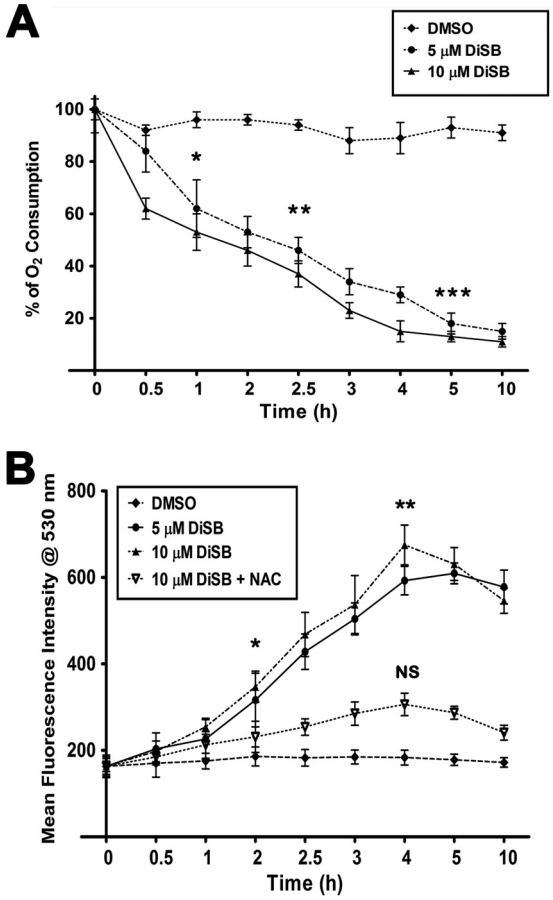

FIG 2 Inhibition of oxygen consumption causes the formation of ROS inside cells. (A) Percentage of inhibition of O_2 consumption was determined after treating the cells in the presence of 0.2% DMSO, 5 μM DiSB, or 10 μM DiSB for periods of 30 min to 10 h, as described in Materials and Methods. The data are normalized with mg of protein and expressed as the mean ± SD values of three independent experiments. (B) Measurement of ROS generation for the promastigotes treated with 0.2% DMSO, 5 μM DiSB, or 10 μM DiSB alone or after preincubation with NAC. After incubation with H_2DCFDA, the fluorescence intensity was measured at 530 nm. The values were obtained in triplicate, averaged, and plotted against time. *, $P < 0.5$; **, $P < 0.05$ (Student's *t* test); ***, $P < 0.005$, which indicates a significant difference between experimental groups and 0-h control. NS, differences are not significant.

hibitor of lipid peroxidation, and subsequently washed and treated with DiSB for the indicated times, the level of fluorescent products decreased as observed after treatment with NAC at 20 μM (Fig. 3C). The abovementioned results suggest that the effect of DiSB is similar to that of CPT with respect to the depletion of GSH level, and it increases the level of lipid peroxidation in leishmanial cells.

DiSB triggers externalization of phosphatidylserine, which is reversed by metacaspase inhibitor. The induction of apoptosis causes the externalization of phosphatidylserine on the surface of apoptotic cells (14), which was detected using annexin V, which binds with exposed phosphatidylserine of the apoptotic cells in a Ca^{2+}-dependent manner. To determine the percentage of apoptotic and necrotic cells in *Leishmania* sp. promastigotes, the cells were incubated with DiSB (10 μM) for 2, 4, 8, or 12 h and then the percentage of cells undergoing apoptosis/necrosis were determined by flow cytometry after staining with annexin V-FITC and PI (Fig. 4A). It is known that dead cells are reactive to PI and that externalized phosphatidylserine residues undergoing apoptosis are detected by annexin V-FITC. Flow cytometric analysis with annexin V/PI staining showed that when cells were exposed to DiSB (10 μM) for 2, 4, or 8 h, the percentage of apoptotic cells increased, with a slight increase in necrotic cells. The proportion of apoptotic and necrotic cells increased from 6 and 1% in the control cells to 38 and 3%, respectively, after treatment with DiSB for 4 h. After 8 h of treatment, the proportions of apoptotic and necrotic cells were increased to 61 and 5%, respectively (Fig. 4A). The number of viable cells decreased from 98 to 13% after treatment with DiSB for 8 h. After treatment with 10 μM DiSB for 12 h, the percentage of the necrotic population increased to 23%, whereas the late-apoptotic/early necrotic population increased to 62%, with only a small population exhibiting annexin V-positive cells (8%). These results suggest that DiSB-induced apoptosis is the main cause of death. The treatment of promastigote cells with 10 μM protease inhibitor (VAD-fmk) for 60 min causes no significant decrease in annexin V positivity, which supports that the appearance of phosphatidylserine on an outer leaflet apparently requires no caspase-like protease activation in *Leishmania* pp. promastigote cells (Fig. 4B). But pretreatment with metacaspase inhibitors, like antipain or TLCK (for 60 min), greatly reduced the apoptotic events induced by DiSB (Fig. 4B), supporting that metacaspase is an effector protease for DiSB-mediated cell death.

DiSB triggers accumulation of intracellular Ca^{2+} pool, followed by depolarization of mitochondrial membrane potential. The morphological changes in PCD result from several physiological imbalances that arise inside the parasites. To confirm that DiSB-induced oxidative stress disrupts the intracellular cation homeostasis of the parasites, the intracellular Ca^{2+} level was estimated. Previous studies have shown that oxidative stress causes mitochondrial depolarization in *L. donovani* by increasing cytosolic Ca^{2+} levels (27). It was also shown that calcium flux is absolutely necessary not only for the activation of different proteases (14) but also for the appearance of phosphatidylserine on the outer leaflet of the plasma membrane during apoptosis. Considering the importance of the cytosolic Ca^{2+} level in inducing apoptosis, we measured the Ca^{2+} concentration in control and DiSB-treated promastigotes at different time intervals. In this study, we have shown that control leishmanial cells maintained intracellular [Ca^{2+}] at 52 ± 7 nM, while DiSB-treated cells exhibited a time-dependent increase in cytosolic [Ca^{2+}] (Fig. 5A). Pretreatment of cells with a selective calcium channel blocker, like verapamil (100 nM), and a nonselective cation channel blocker flufenamic acid (FFA) (250 μM) for 30 min before treatment with DiSB lowered the increase in cytosolic [Ca^{2+}], revealing that both of these channels are affected by treatment with DiSB (Fig. 5A). There was a substantial decrease in the level of intracellular Ca^{2+} during treatment with NAC, suggesting that ROS has an important role in the elevation of intracellular [Ca^{2+}]. The Ca^{2+} ion is an important element in the progression of cell death, as most endonucleases require the presence of Ca^{2+} to cleave DNA strands. Therefore, the molecular mechanism for DiSB-induced apoptosis-like death involves ROS-mediated damage to calcium channels, leading to an increase in the intracellular calcium pool.

The loss of mitochondrial membrane potential is a characteristic feature of metazoan apoptosis associated with the calcium ion imbalance and plays a key role in drug-induced death in *Leishmania* (14). Previous reports on betulin suggest that it induces apop-

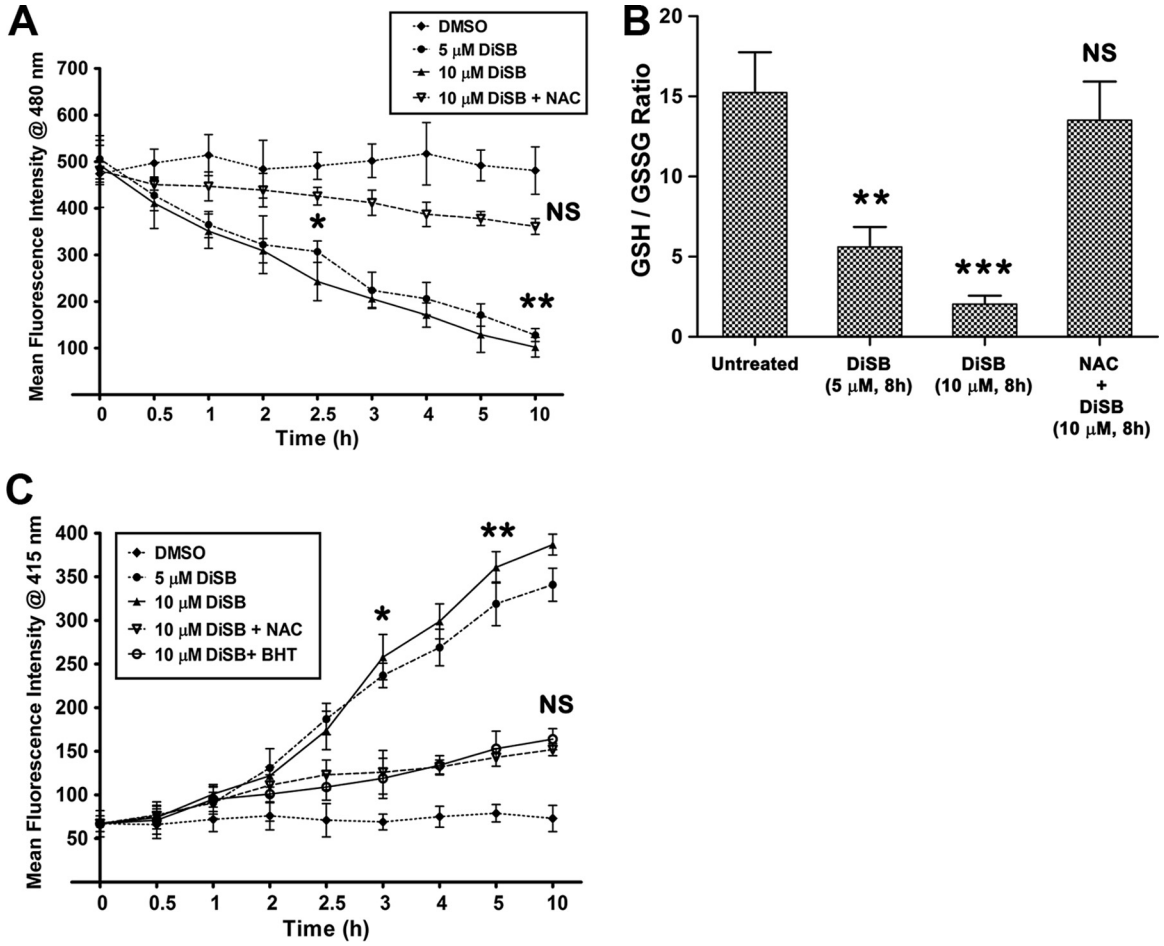

FIG 3 Determination of intracellular GSH level and level of lipid per oxidation during treatment with DiSB. (A) Level of intracellular GSH in *L. donovani* promastigotes in treated and untreated cells. The intracellular GSH level was measured after treatment with DiSB (5 μM or 10 μM), 0.2% DMSO alone, and with NAC prior (30 min) to treatment with DiSB. The intracellular GSH level has been corrected and normalized according to the number of viable parasites. (B) Ratio of GSH to GSSG of DiSB-treated (5 or 10 μM for 8 h) *L. donovani* promastigotes. One set was pretreated with NAC for 60 min, followed by DiSB treatment. (C) The level of fluorescent products of lipid peroxidation was measured after treatment of leishmanial cells with 0.2% DMSO alone, 5 μM DiSB, or 10 μM DiSB and with NAC separately prior to treatment with DiSB. The fluorescence readings were normalized with the total numbers of parasites. The results are the mean ± SD values from three independent experiments. *, $P < 0.5$ (Student's *t* test); **, $P < 0.05$, and ***, $P < 0.01$ compared to DMSO-treated parasites. NS, nonsignificant.

tosis in cancer cells through mitochondrial pathways (30). This prompted us to determine the changes in the mitochondrial membrane potential using the mitosensor dye JC-1. JC-1, a cationic lipophilic dye, becomes concentrated in the mitochondria of healthy cells. This aggregate fluoresces red at higher potentials, but at lower potentials, this reagent cannot accumulate in the mitochondria and remains as a monomer in the cytoplasm that fluoresces green. A fall in the mitochondrial membrane potential increases the green fluorescence intensity. An experiment with JC-1 dye showed accumulation of red signal in the mitochondria of control parasites (Fig. 5B), and the entire cytoplasm colored light green. But when the cells were treated with DiSB, the red signal completely disappeared from mitochondria (Fig. 5B), suggesting that there is a loss of mitochondrial membrane potential. Flow cytometry showed that DiSB-treated parasites exhibit a right shift in the FL-1 channel (Fig. 5C). The mitochondrial uncoupler carbonyl cyanide *m*-chlorophenyl hydrazone (CCCP) (1 μM) caused a greater right shift and served as the positive control. Hence, a loss in $\Delta\psi_m$ was clearly evident. Parasites pretreated with the antioxidant *N*-acetyl cysteine (NAC) for 60 min or the intracellular Ca^{2+} chelator BAPTA-AM [1,2-bis(*o*-aminophenoxy)ethane-N,N,N′,N′-tetraacetic acid] for 30 min, antipain, or TLCK for 60 min prior to DiSB treatment prevented the rapid loss of $\Delta\psi_m$. Hence, DiSB-induced cellular stress alters the calcium homeostasis, which thereby induces a loss of $\Delta\psi_m$. Mitochondrial dysfunction may result through a change in cation homeostasis brought about by high ROS levels (31). The 590:530 ratio was measured through spectrofluorometric analysis. As shown in Fig. 5D, following treatment with 10 μM DiSB, there was a significant fall (61%) in $\Delta\psi_m$ within the first 4 h of treatment with DiSB compared with the relative $\Delta\psi_m$ observed at 0 h. This is concomitant with the ROS production, suggesting that ROS generation precedes the loss of $\Delta\psi_m$. From the above data, it can be inferred that the $\Delta\psi_m$ in promastigotes is sensitive to increasing oxidative stress induced by DiSB treatment. The early loss of potential is indicative of considerable cellular changes taking place soon after the application of oxidative

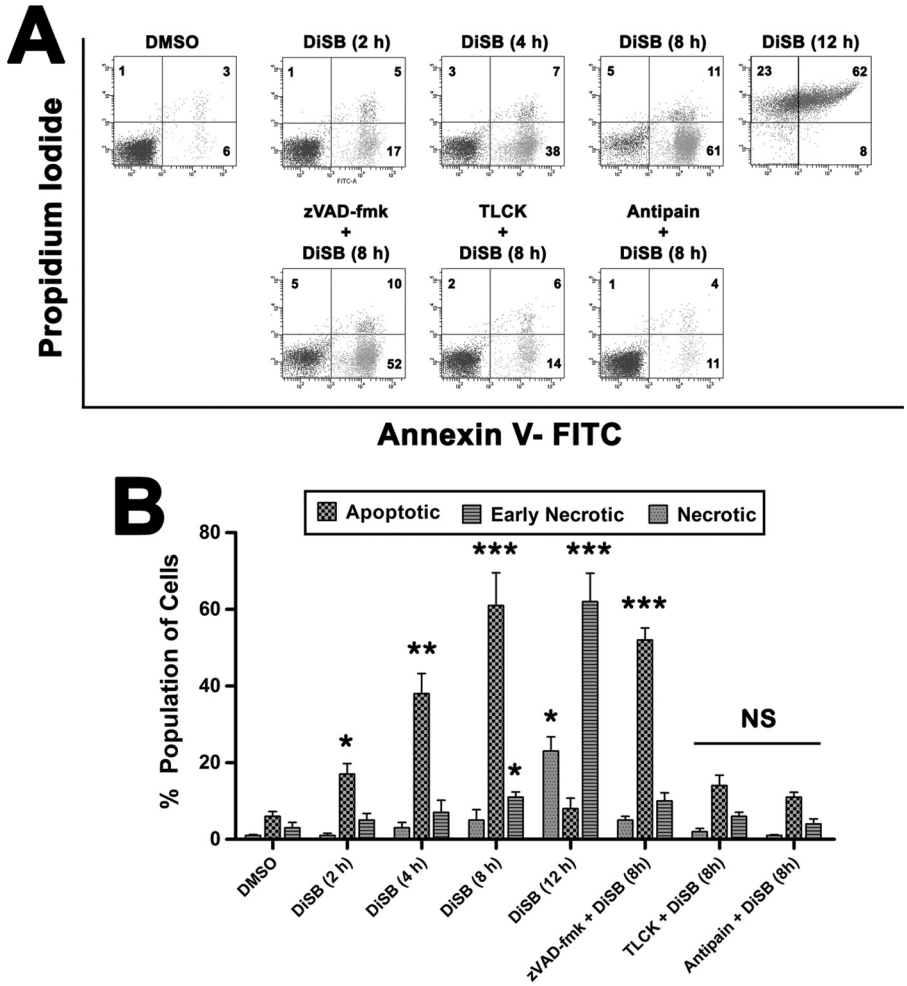

FIG 4 Flow cytometric analysis of promastigote death through PCD/necrotic processes. (A) Externalization of phosphatidylserine was detected in *L. donovani* promastigotes after annexin V labeling of *L. donovani* promastigotes. The cells were treated with 0.2% DMSO alone, with DiSB (10 μM) for 2, 4, 8, or 12 h, with CED3/CPP32 group of protease inhibitors (VAD-fmk), metacaspase inhibitor TLCK, and with antipain (42) for 60 min prior to treatment with DiSB, as described in Materials and Methods. Dot plots are representative of one of three similar results. Apoptotic cells were detected by flow cytometric analysis using annexin V and PI in FL-1 versus FL-2 channels. The cells in the bottom right quadrant indicate apoptosis, whereas cells in the top right quadrant represent the postapoptotic/early necrotic population. (B) Bar graph showing the early apoptotic cells, early necrotic, and necrotic cells as determined by fluorescence-activated cell sorting analysis. The results depicted were performed three times, and representative data from one set of experiments are expressed as mean ± SD values. Variations among different set of experiments were <10%. *, $P < 0.05$ (Student's *t* test), **, $P < 0.01$, ***, $P < 0.001$ compared to DMSO-treated parasites. NS, nonsignificant.

stress. This state of $\Delta\psi_m$ is continued until 4 h of treatment with DiSB. At 8 h of treatment with DiSB, there is a further loss in $\Delta\psi_m$. When cells were treated with the antioxidant NAC before treatment with DiSB, the loss of $\Delta\psi_m$ was only 18% after 8 h of DiSB treatment (Fig. 5D). Similar results were achieved when promastigotes were pretreated with TLCK, antipain, or BAPTA-AM. Since NAC greatly abolished the $\Delta\psi_m$ collapse, these results indicate that the overproduced ROS was responsible for triggering the collapse in mitochondrial potential.

To confirm that the single mitochondrion of *Leishmania* adopts a low energy state when $\Delta\psi_m$ is lowered and a minimum ATP level is maintained to ensure the entry of cells into the apoptotic pathway (27), we measured intracellular ATP content in normal and DiSB-treated parasites. The parasites maintained a higher level of ATP under DMSO-treated conditions (~170.2 nmol/10^8 cells). When treated with 5 μM DiSB for 2 h, the ATP level in the parasites remained almost the same (162.2 nmol/10^8 cells). The dramatic decrease in ATP level has been observed after treatment with DiSB for 4 h, and the level of cellular ATP became about 102.1 nmol/10^8 cells. The treatment of cells for 6 h further decreased the level of ATP to about 68.9 nmol/10^8 cells, and at 8 h of treatment, the ATP level decreased to 21.6 nmol/10^8 cells (Fig. 5E). This confirms that the generation of ROS followed by depolarization of mitochondrial $\Delta\psi_m$ finally hampers cellular ATP generation, which is followed by apoptosis.

DiSB treatment triggers release of cytochrome *c* into the cytosol. Cytochrome *c* is a component of the mitochondrial electron transport chain and is present in the inner membrane. A small amount of cytochrome *c* is present in the cytoplasmic fraction of the control promastigotes. Permeabilization of the mitochondrial outer membrane caused increased release of cytochrome *c* into the cytoplasm with time (Fig. 6A). In case of

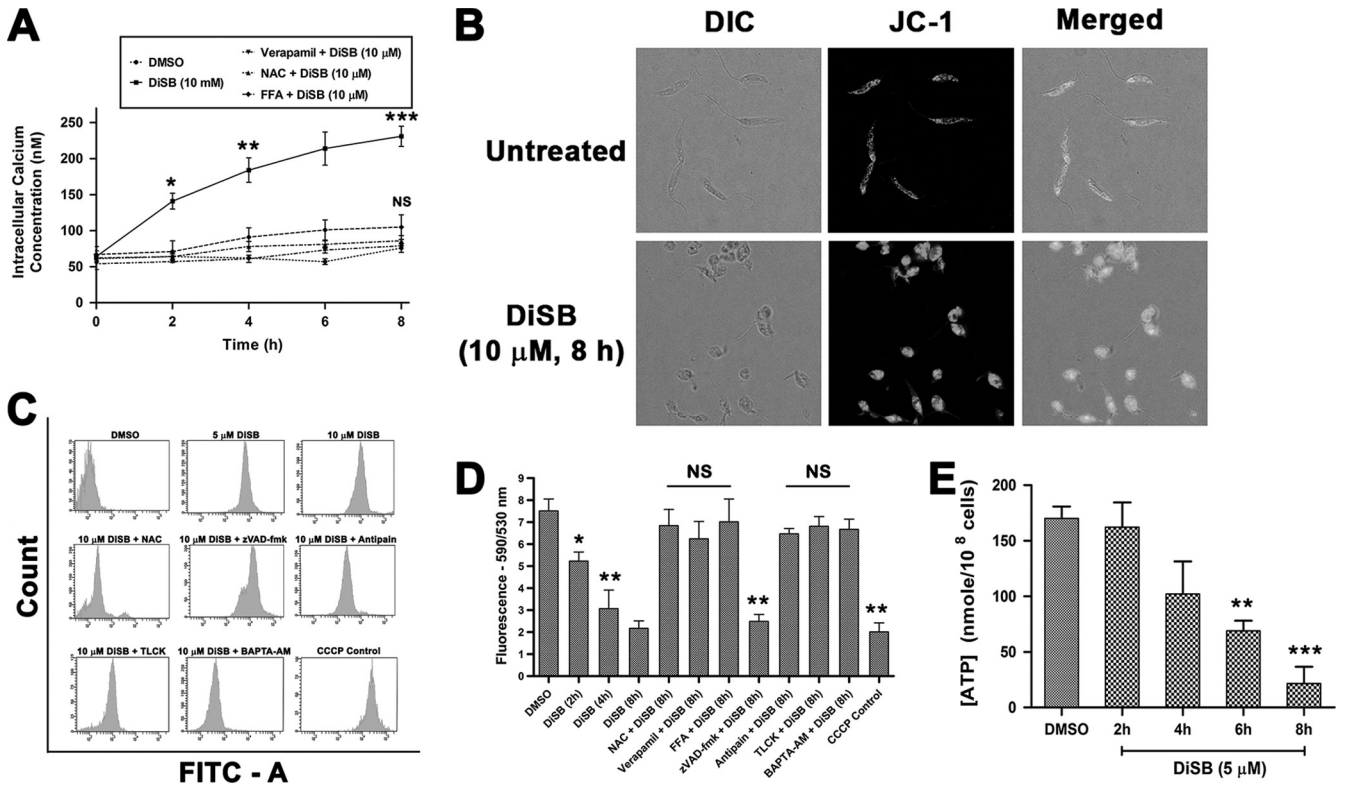

FIG 5 Measurement of DiSB-induced changes in intracellular Ca^{2+} level and mitochondrial membrane depolarization. (A) Increase in Ca^{2+} level was measured after treatment with 10 μM DiSB compared to treatment with 0.2% DMSO alone and with NAC, FFA, or verapamil for 30 min prior to treatment with DiSB. The data were normalized to mg of cellular protein extract. The results are the mean ± SD values from three independent experiments. *, $P < 0.05$ (Student's *t* test); **, $P < 0.01$; ***, $P < 0.001$ compared to DMSO-treated parasites; NS, non significant. (B) Confocal microscopic analysis of JC-1 stain in drug-treated or untreated *L. donovani* cells. In normal cells, the cytoplasm stains as light green and mitochondria as red. In case of DiSB-treated cells, the red color disappears, and the total cell appears green. For each set, the differential inference contrast (DIC), red/green merged channel, and DIC merged pictures were provided. (C) Flow cytometric analysis of mitochondrial membrane potential. The parasites were treated with 0.2% DMSO, DiSB (5 or 10 μM), CCCP (1 μM), or with 10 μM DiSB after pretreatment with NAC, BAPTA-AM, zVAD-fmk, antipain, or TLCK (60 min), as mentioned in Materials and Methods. Thereafter, promastigotes were incubated with BD mitosensor reagent and the green fluorescence intensity was monitored using flow cytometry. (D) *L. donovani* promastigotes were exposed to 0.2% DMSO, 10 μM DiSB for 2 h, 4 h, and 8 h and pretreated for 60 min with 20 μM NAC, 240 μM FFA, 100 nM verapamil, zVAD-fmk, antipain, TLCK, or BAPTA-AM separately before treatment with DiSB for 8 h and subsequently stained with the potentiometric probe JC-1 (10 μM). The relative $\Delta\psi_m$ values are expressed as the ratio of the reading at 590 nm (aggregate) to the reading at 530 nm (monomer). The data are the mean ± SD values from three independent experiments. *, $P < 0.5$ (Student's *t* test); **, $P < 0.01$ compared to DMSO-treated parasites; NS, nonsignificant. (E) *L. donovani* promastigotes were exposed to 0.2% DMSO, 5 μM DiSB for 2 h, 4 h, 6 h, or 8 h, and total cytosolic ATP was measured as described in Materials and methods. The data are the mean ± SD values from three independent experiments. **, $P < 0.5$ (Student's *t* test), and ***, $P < 0.01$ compared to DMSO-treated parasites.

untreated promastigotes, the punctate cytochrome *c* resides in the mitochondria. Treatment with DiSB rapidly translocated cytochrome *c* into the cytosol (Fig. 6A). This cytosolic efflux of cytochrome *c* is concomitant with a reciprocal decrease in mitochondrial cytochrome *c* (Fig. 6B). The pretreatment of the parasites with NAC, BAPTA-AM, antipain, or TLCK decreased the rate of cytochrome *c* release. However, pretreatment of the parasites with the caspase inhibitor, zVAD-fmk, for 60 min did not prevent rapid cytochrome *c* release (Fig. 6C). Disruption of the outer mitochondrial membrane by apoptotic stimuli results in the release of the cytochrome *c* into the cytoplasm, which activates a cascade of proteases involved in apoptosis.

DiSB causes activation of noncanonical metacaspase proteases. Metacaspases are caspase-related cysteine-proteases that are present in organisms without caspases, such as plants, yeast, and protozoan parasites. Since caspases are important effector molecules in mammalian apoptosis, the possible role of metacaspases in PCD was evaluated in the *L. donovani* promastigotes after treatment with DiSB. Our data suggest that programmed cell death cannot be reversed by pretreatment with caspase inhibitors but is inhibited by metacaspase-specific inhibitors. In order to compare the level of LdMC (metacaspase) activity in the drug-treated promastigotes, enzyme assays were done with lysates of promastigotes harvested in mid-log growth phase and using Boc-GRR-AMC as the substrate. The expression levels of metacaspase were detected at 4 and 8 h posttreatment with DiSB (Fig. 7A). Untreated cells expressed metacaspase genes steadily at several time points. Our results showed an increase in the activity of LdMC in parasites treated with DiSB compared to untreated controls (Fig. 7A).

To further support the potential role of LdMCs in DiSB-triggered apoptosis, parasites were transfected with conditional antisense construct of LdMC, in which antisense mRNA is produced under the control of the Tet repressor gene. DiSB was added to parasites after 24 h of Tet-induced or -uninduced pLew82 (empty vector), and anti-MC transfectants and the percentage of live pro-

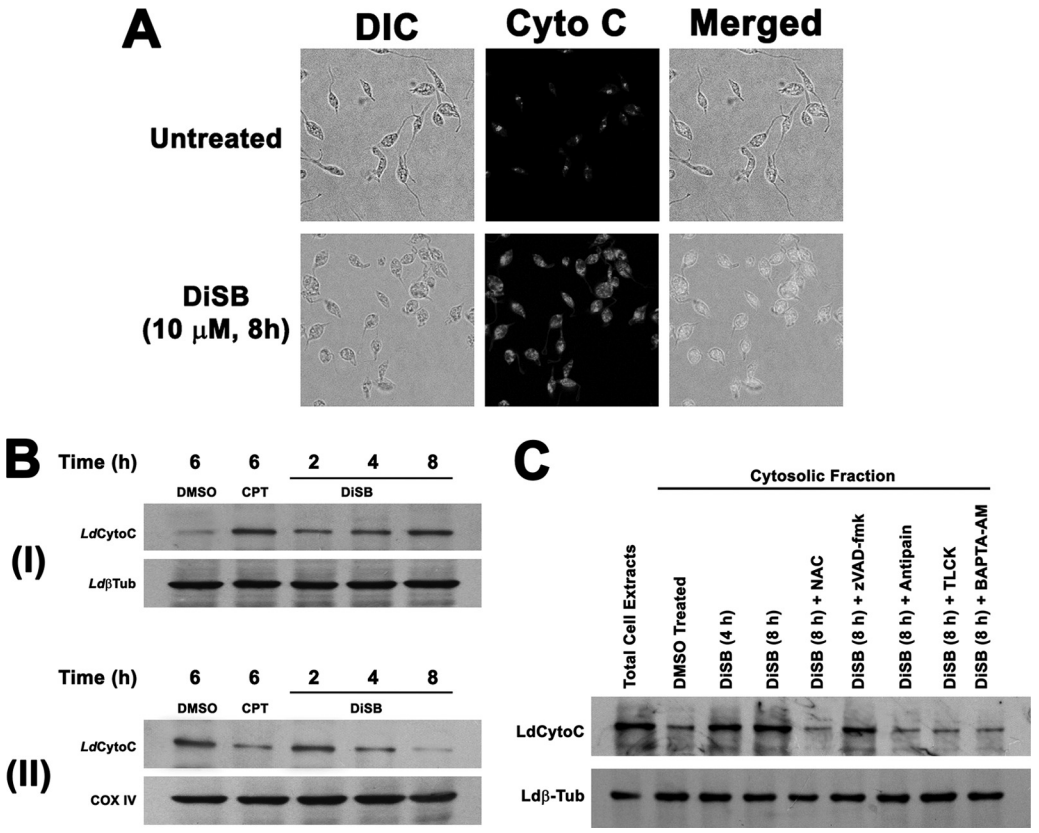

FIG 6 Determination of cytochrome *c* release in DiSB-treated *L. donovani* promastigotes. (A) Localization of cytochrome *c* in treated and untreated cells through confocal microscopy. *Leishmania* cells were treated with 0.2% DMSO and DiSB (10 μM). After 8 h, the cells were smeared and fixed with 3.7% paraformaldehyde, followed by permeabilization with 0.1% Triton X-100. The cells were incubated overnight with anti-cytochrome *c* antibody, counterstained with FITC-conjugated secondary antibody, and confocal microscopic pictures were taken. The pictures are representative of one of three similar results. (B) Western blot analysis to detect the levels of cytochrome *c* for cytoplasmic (panel I) and mitochondrial (panel II) fractions from parasites taken at the given times of differently treated cells. Lane 1, cytosolic level of cytochrome *c* in DMSO-treated leishmanial cells; lane 2, CPT-treated (6 h) leishmanial cells; lanes 3 to 5, cells treated with DiSB (10 μM) for 2, 4, or 8 h, respectively. Immunoblots of Ldβ-tubulin and LdCOXIV served as loading controls for the cytosolic and mitochondrial fractions, respectively. (C) Immunoblot for cytochrome *c* in total cell lysate (lane 1), cytosolic extracts from 0.2% DMSO-treated parasites (lane 2), DiSB (10 μM) treated for 4 h (lane 3) and 8 h (lane 4), DiSB-treated parasites after pretreatment with 20 μM NAC (lane 5), 25 μM zVAD-fmk (lane 6), 2 μM antipain (lane 7), 10 μM TLCK (lane 8), or 25 μM BAPTA-AM (lane 9). An immunoblot using anti-β-tubulin antibody served as the loading control.

mastigotes were plotted against the time after DiSB treatment (Fig. 7B). The treatment of LdMC-downregulated parasites (anti-MC) with DiSB induced a slow death, while DiSB treatment of other parasites induced LdMC-mediated PCD progression. DNA fragmentations were considerably reduced in DiSB-treated LdMC-downregulated parasites (Fig. 7C). Therefore, the absence of effector metacaspases in anti-MC parasites generates a negative feedback response, which suppresses the signaling cascades in the parasites.

DiSB-induced DNA fragmentation is associated with LdEndoG activation. The internucleosomal DNA digestion by an endogenous nuclease (genomic DNA fragmentation) is considered to be a hallmark of apoptotic cell death (32). To establish the DiSB-induced DNA fragmentation, we performed the DNA fragmentation assay by a DNA laddering experiment. DMSO-treated parasites exhibited a single genomic DNA band, whereas DiSB-treated parasites showed a laddering pattern indicative of DNA fragmentation. H_2O_2-treated parasites exhibit more prominent ladders (Fig. 8A). DNA fragmentation assay using ELISA showed that DiSB treatment of parasites along with antipain caused a 42% reduction in DNA fragmentation in 4 h. It was observed that there was 45 and 76% fragmentation of DNA by treatment with DiSB (10 μM) at 4 and 8 h, respectively (Fig. 8B). The drug concentration (10 μM) used has been optimized on the basis of the percentage of DNA fragmentation induced at 8 h of drug treatment. Further treatment with the drug for 12 h did not increase DNA fragmentation (data not shown), and it remains almost same as before (79%). Treatment with the protease inhibitor VAD-fmk (25 μM) had no effect on DNA fragmentation, but the antioxidant NAC, metacaspase inhibitor antipain, and endonuclease G (Endo G) inhibitor ATA reduced the percentage of DNA fragmentation. Therefore, these results indicate that caspase-like protease has no role in DiSB-mediated PCD, but metacaspases, as well as LdEndoG and ROS, are also responsible for DNA fragmentation in DiSB-induced cell death. *Leishmania* parasites exhibit stress-induced activation of metacaspases, which thereby induce DNA fragmentation.

PARP is an enzyme involved in DNA repair when DNA damage is sensed (33). PARP cleavage was studied after the treatment of *L. donovani* promastigotes with 10 μM DiSB for various time periods. The expression of PARP was detected in the cells at 2, 4, and 8 h posttreatment (Fig. 8C). The PARP protein (78 kDa)

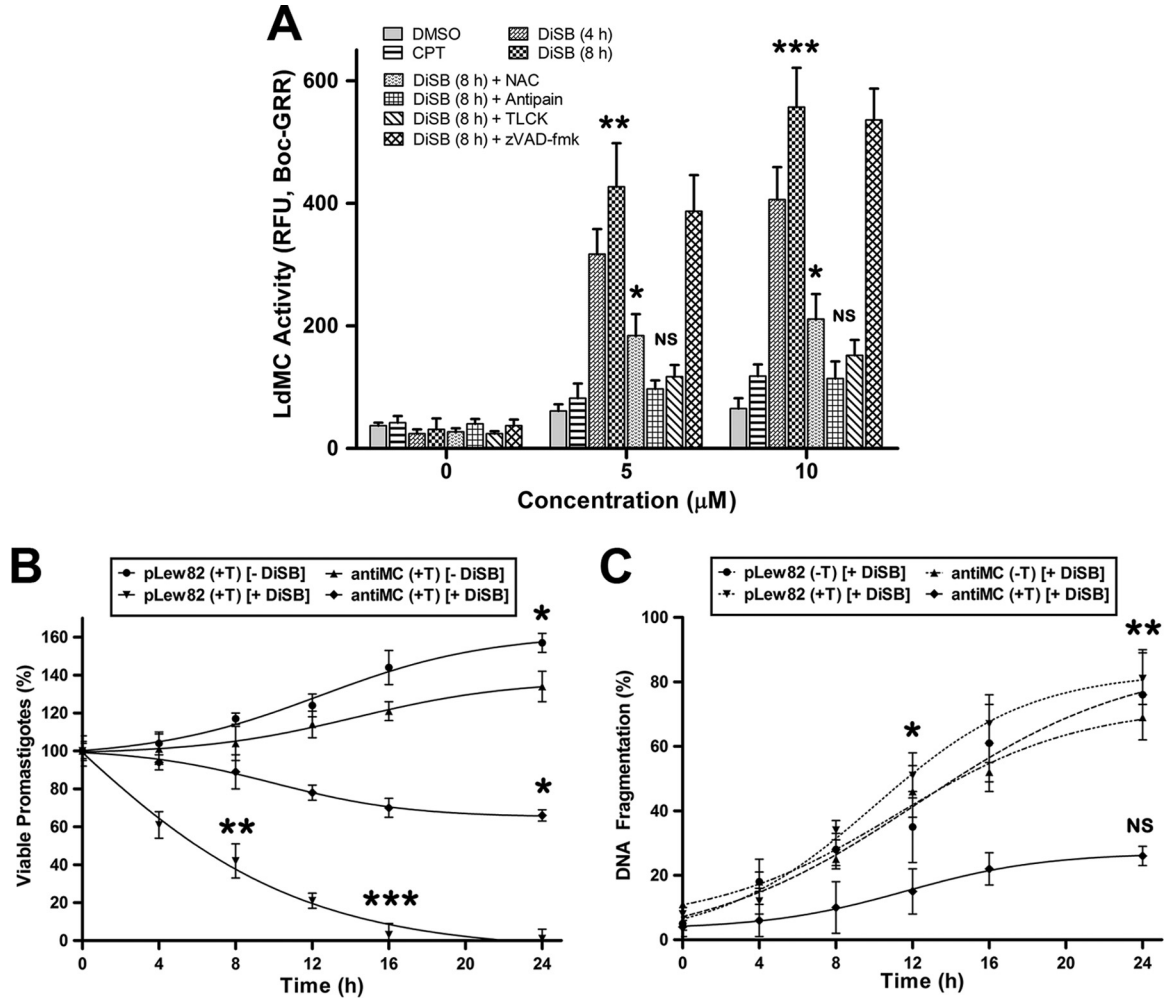

FIG 7 Determination of metacaspase activity and its downstream effects in the presence and in the absence of protease inhibitor. (A) Activation of metacaspases in the cytosol of leishmanial cells was measured after treatment with 0.2% DMSO, 5 μM CPT alone, DiSB (10 μM) alone for 4 or 8 h, or with NAC, antipain, TLCK, or CED3/CPP32 group of inhibitor zVAD-fmk pretreated (for 60 min) cells. Metacaspase activity was measured using Boc-GRR-AMC as the substrate and expressed in relative fluorescence units (RFU) and normalized to mg of protein of cellular extracts. The bar represents the averages of three independent assays. Standard deviations (error bars) are shown. (B) Viability of LdMC knocked down parasites upon DiSB treatment. Transfectants, pLew82, and anti-MC were induced by Tet (+T) for 24 h and thereafter treated with 10 μM DiSB or without for 24 h. The percentages of viable promastigotes were calculated using AlamarBlue reagent. The values taken in triplicate were averaged and plotted against time. (C) Extent of DNA fragmentation upon DiSB treatment for 24 h in cells transfected with pLew82 or with anti-MC. The transfectants were induced with Tet or without for 24 h prior to treatment with DiSB. The values were obtained from the Multiskan EX readings at 405 nm. The percentages were plotted versus time. The data represent the mean ± SD values ($n = 3$). *, $P < 0.05$ (Student's *t* test), **, $P < 0.01$, and ***, $P < 0.001$ compared to DMSO-treated parasites. NS, nonsignificant.

generates a 63-kDa cleaved fragment upon the treatment of cells with DiSB for 4 and 8 h, and the extent of PARP cleavage is greater at 8 h. However, the cleavage of this PARP protein did not occur when cells were pretreated with antipain or the endonuclease inhibitor ATA.

Immunoblotting with anti-LdEndoG for mitochondrial and nuclear extracts prepared from parasites showed a gradual translocation of LdEndoG to the nucleus with increasing time after treatment with DiSB (Fig. 8D). The equal band intensities corresponding to LdCOXIV for the mitochondrial extracts and LdHistone H1 for the nuclear extracts served as loading controls.

Terminal deoxynucleotidyl transferase-mediated dUTP nick-end labeling (TUNEL) assays helped to visualize the efficacy of these inhibitors in preventing DiSB-induced DNA fragmentation. Figure 8E shows the time course increase (24% in 2 h and 77% in 8 h) in DNA fragmentation upon DiSB treatment, as evident from the flow cytometry analysis. zVAD-fmk did not prevent DiSB-induced DNA fragmentation; hence, parasites were TUNEL positive (72%). Parasites pretreated with ATA (30 min) or antipain (60 min) prior to DiSB treatment showed reduced (15 to 18%) TUNEL-positive parasites, as they inhibit the DiSB-activated endonucleases. Microscopic analysis also revealed that the number of TUNEL-positive nuclei is reduced following antipain pretreatment (Fig. 8F). Thus, DiSB-induced oxidative stress activates endonucleases and is independent of caspase-like proteins in these parasites. The concomitant increase in metacaspase activity and percentage of TUNEL-positive cells in parasites treated with DiSB suggest a possible involvement of LdMCs in DiSB-induced *Leishmania* PCD.

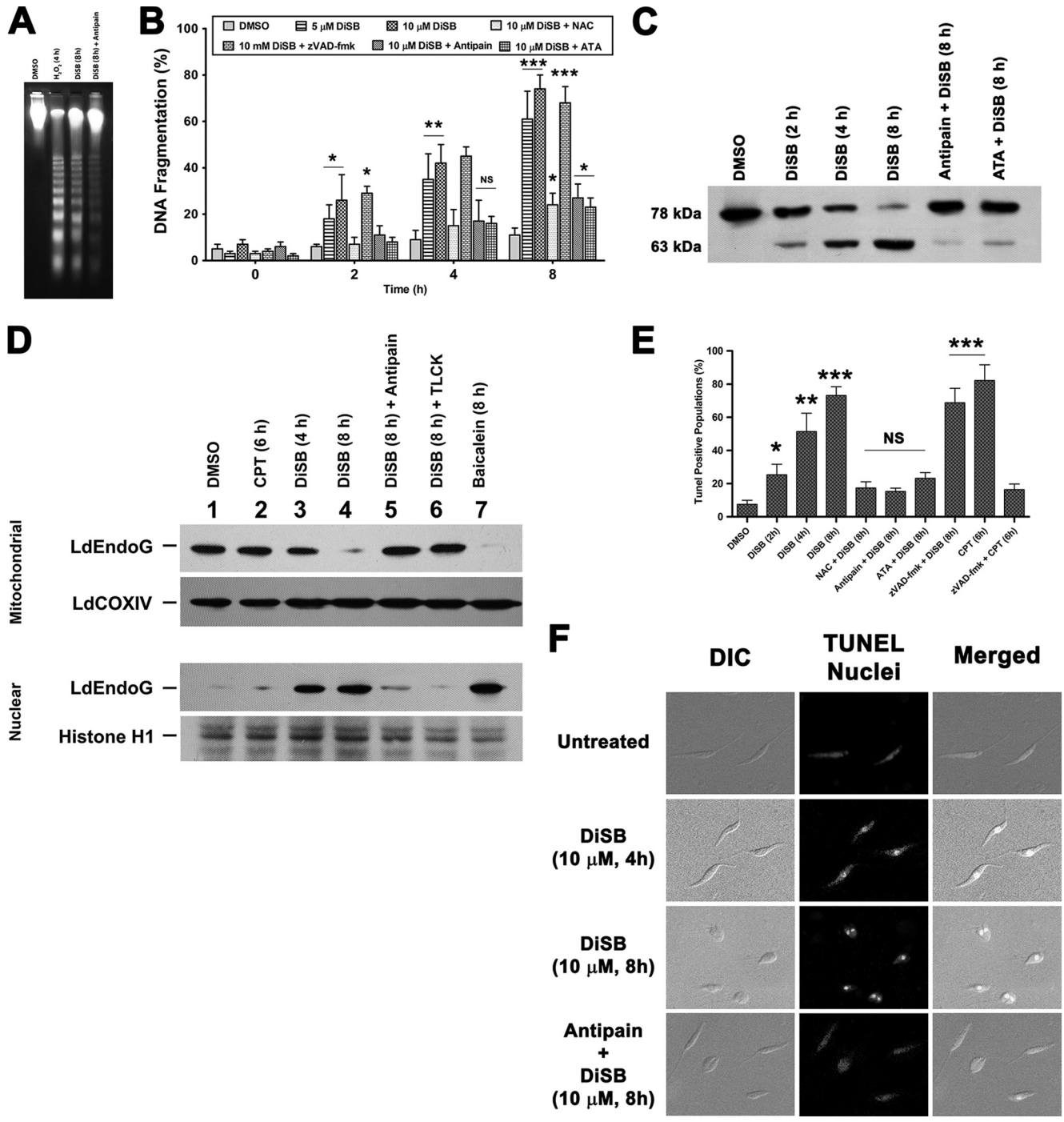

FIG 8 DiSB-induced DNA fragmentation assay with activation of cellular endonuclease. (A) Genomic DNAs were isolated from *L. donovani* promastigotes after treatment with 0.2% DMSO, 5μM H_2O_2 for 4 h, 10 μM DiSB for 8 h, or 10 μM DiSB along with 2 μM antipain. (B) Extent of genomic DNA fragmentation upon DiSB treatment. Parasites were treated with 5 μM or 10 μM DiSB alone or after preincubation with NAC, 25 μM zVAD-fmk, or 2 μM antipain. As a negative control, the parasites were also treated with 0.2% DMSO. The values were obtained from the Multiskan EX readings at 405 nm and normalized to the total number of cells. The relative percentage (with respect to samples treated with micrococcal nuclease and normalized to percentage values) was plotted as units of time. The data represent the mean ± SD values ($n = 3$). *, $P < 0.5$ (Student's *t* test), **, $P < 0.05$, and ***, $P < 0.01$ compared to DMSO-treated parasites; NS, nonsignificant. (C) Western blot analysis to detect the cleavage of full-length PARP protein after treatment with 0.2% DMSO (lane 1), DiSB (10 μM) for 2 h, 4 h, or 8 h (lanes 2, 3, and 4, respectively), or with the metacaspase group of protease inhibitor (antipain) before treatment with DiSB (lane 5) or with endonuclease G inhibitor ATA (lane 6). (D) Nuclear translocation of LdEndoG. Western blot analysis of the mitochondrial and nuclear fractions obtained from DiSB-treated parasites at different intervals or pretreated with antipain (for 60 min) and ATA (for 30 min); baicalein treatment served as a positive control. Immunoblotting with anti-LdEndoG showed a gradual decrease in LdEndoG from the mitochondrial fraction, with a concomitant increase in the nuclear fraction, anti-COXIV, and anti-histone H1, which served as the loading controls for the mitochondrial and nuclear fractions. (E) DiSB-induced DNA fragmentation was analyzed by TUNEL assay using flow cytometry. The parasites were treated with 0.2% DMSO or 10 μM DiSB for 4 or 8 h. DiSB treatment was also carried out after preincubation with NAC (60 min), 25 μM zVAD-fmk (60 min), 2 μM antipain (60 min), or 50 μM ATA (30 min). Treatment with CPT (10 μM) alone or after preincubation with 25 μM zVAD-fmk served as a positive control. A graphical representation of the percentage of TUNEL-positive nuclei is plotted. The mean values for three sets of 10,000 parasites were plotted. *, $P < 0.05$ (Student's *t* test), and **, $P < 0.01$ compared to DMSO-treated parasites. NS, nonsignificant. (F) DiSB-induced DNA cleavage was characterized in *L. donovani* promastigote cells by a TUNEL assay. Nonapoptotic cells (untreated), cells after treatment with 10 μM DiSB for 4 h or 8 h, or with metacaspase inhibitor (antipain) were visualized. PI was added as a counter stain.

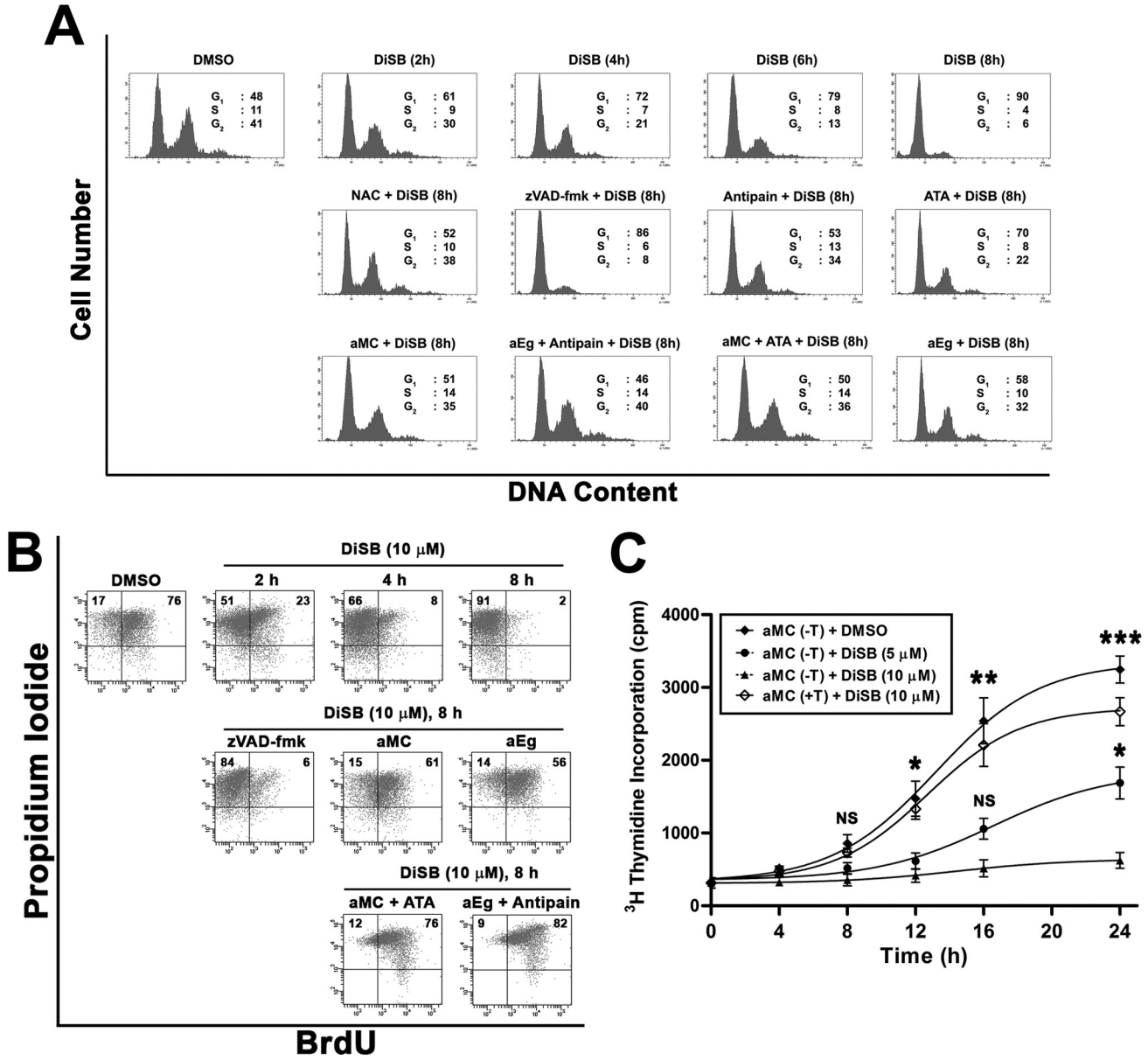

FIG 9 Subversion of cell cycle arrest in LdMC-knockdown parasites upon DiSB treatment and analysis of DNA synthesis in DiSB-treated parasites. (A) DiSB-mediated cell cycle arrest in *L. tarentolae* promastigote cells. Histograms of distribution of DNA content with flow cytometry in *Leishmania* cells are shown. Cell cycle arrest was analyzed after treatment with 0.2% DMSO as control, and with DiSB (10 μM) for 2, 4, 6, and 8 h or pretreated with different inhibitors, like NAC, zVAD-fmk, antipain, or ATA. The cells were then fixed and stained with propidium iodide, and the nuclei were analyzed for DNA content by flow cytometry. In another set, an antisense construct of EndoG and metacaspase was transfected individually or with antipain and ATA and were analyzed. In total, 20,000 nuclei were counted from each sample. The percentages of cells within different cell stages were determined as described in Materials and Methods. (B) Flow cytometric analysis of DNA synthesis was performed by BrdU incorporation as per the manufacturer's protocol (Roche Bioscience). After different treatments (as shown), the cells were fixed with ethanol and anti-BrdU antibody was used, followed by FITC-conjugated secondary antibody. Finally, the cells were incubated with propidium iodide (with RNase A). All the experiments were performed three times, and the results of one such experiment was given. (C) Incorporation of [^{3}H]-thymidine (5 μCi/ml) into DNA of *L. tarentolae* cells. Incorporation was monitored at different times after addition of [^{3}H]-thymidine and 0.2% DMSO, followed by the addition of DiSB (5 μM or 10 μM for 24 h) in Tet-uninduced (−T) antisense construct of metacaspase (aMC)-transfected promastigotes, or with Tet-induced (+T) antisense constructs. Aliquots of 200 μl each were withdrawn from the cultures at the indicated time intervals and processed to determine the incorporation of label into acid-precipitable DNA and normalized to total number of promastigotes. The experiments were performed three times, and the representative data from one set of these experiments are presented as the mean ± SD values. The variations among the different sets of experiments were <8%. *, $P < 0.5$ (Student's *t* test), **, $P < 0.05$, and ***, $P < 0.01$ compared to DMSO-treated controls. NS, nonsignificant.

Conditional knockdown of LdMC and LdEndoG bypasses *Leishmania* cell cycle arrest and DNA synthesis followed by DiSB treatment. The cell cycle distribution was analyzed by flow cytometry after treatment with DiSB for different amounts of time (Fig. 9A). In control cells, the G_1, S, and G_2/M populations remained almost the same. DiSB caused *L. tarentolae* promastigotes to remain at resting G_0/G1 phase and inhibited their entry into the S phase. The flow cytometric experiment showed that 90% of the

cells were in G_1 phase, whereas 4% and 6% were in S phase and G_2/M phase, respectively, after treatment with DiSB (10 μM) for 8 h. Treatment with NAC, antipain, or ATA overcame the cell cycle arrest, whereas the caspase inhibitor had less effect on the reversal. Anti-MC and anti-Eg transfectants easily bypassed the arresting step. Arrest of the cell cycle was reversed almost to untreated control levels when we used endonuclease G inhibitor ATA on anti-MC transfectants, and vice versa, proving that both metacaspase and endonuclease G are key effector molecules that trigger DiSB-mediated cell death.

The effect of DiSB on DNA synthesis was studied by the incorporation of BrdU (Fig. 9B) and [^{3}H]thymidine into DNA (Fig. 9C) of *L. tarentolae* promastigotes in the presence and absence of different concentrations of DiSB. Treatment with DiSB at 10 μM for 2, 4, and 8 h decreased the BrdU incorporation and [^{3}H]thymidine incorporation in promastigotes. After 24 h of incubation with 5 and 10 μM DiSB, the [^{3}H]thymidine incorporation rates decreased by 52 and 85%, respectively. The decrease in the rate of thymidine incorporation with time at a particular concentration indicates a decrease in DNA replication activity within the parasites. When antisense constructs of MC were transfected to *L. tarentolae* parasites, it reverted the DNA synthesis inhibition by almost 82% (Fig. 9C). This was concomitant with the BrdU incorporation. Transfectants of anti-metacaspase and EndoG relieved the DiSB-mediated cell cycle arrest. The reversal was almost similar to that of untreated cells when endonuclease G inhibitor ATA was used on anti-MC transfectants, and vice versa.

DISCUSSION

Although the PCD of unicellular organisms has been established (34, 35), the pathway in protozoan parasites has not been well characterized. A search in the *Leishmania* genome database failed to identify most of the effector molecules associated with the caspase-dependent PCD pathway. A recent report identified Endo G of kinetoplastids as an effector molecule of the kinetoplastid PCD pathway (36), but the initiation of PCD has not been clearly understood. Recently, metacaspases have come up as effector molecules in these parasites (37). We have shown previously that DiSB directly interacts with topoisomerase I, thus inhibiting all the life processes associated with double-stranded DNA (dsDNA) transactions in leishmanial cells, and it acts as a catalytic inhibitor of topoisomerase I (18). CPT, a potent antitumor agent, can trap topoisomerase I-mediated cleavable complex in the mitochondria (38) and increases the cellular ROS generation in leishmanial cells (14).

In the present study, we found an inhibition in the growth of *L. donovani* promastigotes by DiSB in a dose-dependent manner. In accordance with previous studies on betulin, a significant population of the leishmanial cells in G_2/M phase was decreased when parasites were exposed to 10 μM DiSB. The present study indicates that DiSB was an effective inducer of apoptosis in *L. donovani*, and that is confirmed by phosphatidylserine externalization and DNA fragmentation. An established event in most apoptotic cells is the generation of ROS in the cytosol that directs the cell toward the path of death. Because DiSB interacts with topoisomerase I, it might generate ROS inside mitochondria. Therefore, we measured the endogenous ROS in leishmanial cells after treatment with DiSB. It was found that there was a consistent increase in cytosolic ROS. However, pretreatment with NAC did not revert the ROS level to a normal state. This may be due to the topoisomerase lesions that DiSB generates inside parasites, which becomes irreversible.

DiSB-induced oxidative stress increases the intracellular calcium ion concentration, which concomitantly accumulates in the mitochondria. Cation imbalance inside the parasite mitochondria causes its membrane to depolarize. When the calcium concentration reaches a critical threshold, the mitochondrial outer membrane is permeabilized (mediated by voltage-dependent anion channel [VDAC]) (29). Increased ROS production depletes cellular GSH levels in *Leishmania* and thereby accelerates growth arrest. There is concomitant inner membrane permeabilization, promoted by the permeability transition pore. The resulting generation of ROS boosts the stress pathway and also causes oxidative DNA lesions (39), which are generated by abrogating topoisomerase DNA interactions. Lipid peroxidation causes the release of cytochrome *c* into the cytosol along with the effector endonuclease, LdEndoG (14). ATA inhibits the effector endonuclease and generates a negative feedback response to arrest the interlinked signaling cascade and help maintain cation homeostasis (40).

There was a depletion of the mitochondrial ATP level in the DiSB-treated cells, and the extent of depletion within 30 min was almost 20%, which increased to almost 60% in 4 h. An almost similar type of mitochondrial ATP depletion was observed in oligomycin-treated cells (data not shown). The abovementioned results suggest that mitochondrial ATP depletion after treatment with DiSB is due to the inhibition of mitochondrial oxidative phosphorylation. In the absence of proper functional mitochondria, cells cease to synthesize ATP from their mitochondrial source and cause a rapid decrease in cellular ATP levels to the extent of 53% by 120 min. Our results are consistent with those of the study reported previously that the ATP level gradually decreases after the loss of $\Delta\psi_m$ during treatment with H_2O_2 (27). However, ATP is a key molecule for chromatin condensation, nuclear fragmentation and regulation, and the maintenance of ion homeostasis during apoptosis. Therefore, we can assume that the ATP levels generated before the loss of $\Delta\psi_m$ and the ATP supplied by glycolysis are sufficient to carry out these cellular activities and to propagate PCD in leishmanial cells.

In higher eukaryotes, the release of cytochrome *c* results in an apoptosome formation that activates the caspase cascade and therefore caspase-activated DNases (CAD) (41). The negative assays for caspase-like proteins (data not shown), ineffectiveness of zVAD-fmk, and activity of Boc-GRR-AMC indicated the activation of a metacaspase-dependent PCD mechanism by DiSB. DiSB treatment translocates LdEndoG into the nucleus, which, along with ROS, produces nicked chromatin. Besides, DiSB generates single- and double-strand breaks by trapping DNA topoisomerases (18). This nicked chromatin forms the substrate of an LdEndoG-assembled DNA "degradosome" complex (25). DiSB-treated *Leishmania* parasites activate metacaspase, and downregulation to this metacaspase subverts cell death. Most mammalian caspases are synthesized as catalytically inactive zymogens that are processed into active proteases upon activation of the cell death pathway. *L. donovani* metacaspases do not appear to be processed under normal growth conditions or upon treatment with inducers of PCD (42). This suggests that LdMCs can be synthesized in active forms and that the parasites must have a mechanism(s) to control/isolate metacaspase activity inside the cell.

In conclusion, DiSB-induced apoptosis appears to be primarily associated with the early activation of metacaspase through the

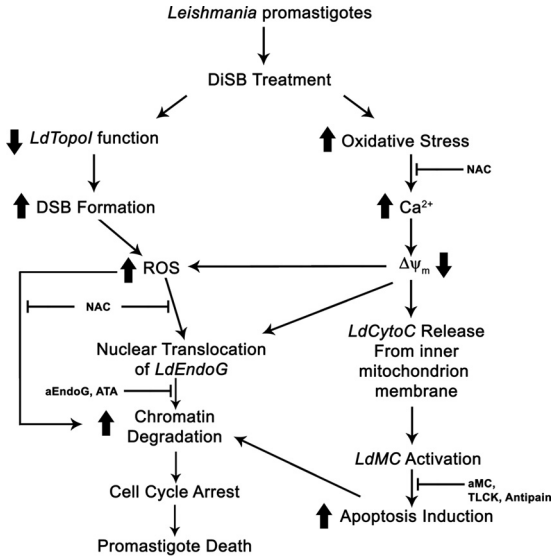

FIG 10 Schematic pathway of DiSB-induced metacaspase-dependent programmed cell death in *Leishmania* involving a LdEndoG.

mitochondrial pathway, as demonstrated by the simultaneous loss of mitochondrial membrane potential and the consequent release of cytochrome *c* (Fig. 10). As a specific target to topoisomerase type IB of *Leishmania* promastigotes, DiSB has the potency to be developed for antileishmanial drugs (18). Exploiting the mechanistic understanding of the selective cytotoxic effect of DiSB on *Leishmani*a respiting host cells may aid in the development of novel and potent chemotherapeutic agents accompanied by diminished side effects.

ACKNOWLEDGMENTS

We thank S. Roy (Director of Indian Institute of Chemical Biology, Kolkata, India) for interest in this work. We thank Rupkatha Mukhopadhyay for flow cytometry analysis.

S. Chowdhury, S. Sengupta, and H. K. Majumder participated in the research design, S. Chowdhury, S. R. Chowdhury, and T. Mukherjee conducted experiments, T. Mukherjee and P. Jaisankar contributed new reagents or analytic tools, S. Chowdhury and H. K. Majumder performed data analysis, and S. Chowdhury and H. K. Majumder wrote or contributed to the writing of the manuscript.

This work was supported by grants from the Network Project from the Council of Scientific and Industrial Research (CSIR), the Government of India (grant NWP-0038) and the DBT Project (grant BT/PR4456/MED/29/355/2012) of the Government of India.

REFERENCES

1. **Nguewa PA, Fuertes MA, Valladares B, Alonso C, Pérez JM.** 2004. Programmed cell death in trypanosomatids: a way to maximize their biological fitness? Trends Parasitol. **20:**375–380. http://dx.doi.org/10.1016/j.pt.2004.05.006.
2. **Savill J, Fadok V.** 2000. Corpse clearance defines the meaning of cell death. Nature **407:**784–788. http://dx.doi.org/10.1038/35037722.
3. **Martinvalet D, Zhu P, Lieberman J.** 2005. Granzyme A induces caspase-independent mitochondrial damage, a required first step for apoptosis. Immunity **22:**355–370. http://dx.doi.org/10.1016/j.immuni.2005.02.004.
4. **Li LY, Luo X, Wang X.** 2001. Endonuclease G is an apoptotic DNase when released from mitochondria. Nature **412:**95–99. http://dx.doi.org/10.1038/35083620.
5. **Ishihara Y, Shimamoto N.** 2006. Involvement of endonuclease G in nucleosomal DNA fragmentation under sustained endogenous oxidative stress. J. Biol. Chem. **281:**6726–6733. http://dx.doi.org/10.1074/jbc.M510382200.
6. **Kobets T, Grekov I, Lipoldova M.** 2012. Leishmaniasis: prevention, parasite detection and treatment. Curr. Med. Chem. **19:**1443–1474. http://dx.doi.org/10.2174/092986712799828300.
7. **Kaye P, Scott P.** 2011. Leishmaniasis: complexity at the host-pathogen interface. Nat. Rev. Microbiol. **9:**604–615. http://dx.doi.org/10.1038/nrmicro2608.
8. **Ashutosh, Sundar S, Goyal N.** 2007. Molecular mechanisms of antimony resistance in *Leishmania*. J. Med. Microbiol. **56:**143–153. http://dx.doi.org/10.1099/jmm.0.46841-0.
9. **Debrabant A, Nakhasi H.** 2003. Programmed cell death in trypanosomatids: is it an altruistic mechanism for survival of the fittest? Kinetoplastid Biol. Dis. **2:**7. http://dx.doi.org/10.1186/1475-9292-2-7.
10. **Chowdhury S, Mukherjee T, Mukhopadhyay R, Mukherjee B, Sengupta S, Chattopadhyay S, Jaisankar P, Roy S, Majumder HK.** 2012. The lignan niranthin poisons *Leishmania donovani* topoisomerase IB and favours a Th1 immune response in mice. EMBO Mol. Med. **10:**1126–1143. http://dx.doi.org/10.1002/emmm.201201316.
11. **Sordet O, Khan QA, Kohn KW, Pommier Y.** 2003. Apoptosis induced by topoisomerase inhibitors. Curr. Med. Chem. Anticancer Agents **3:**271–290. http://dx.doi.org/10.2174/1568011033482378.
12. **Barry M, Bleackley RC.** 2002. Cytotoxic T lymphocytes: all roads lead to death. Nat. Rev. Immunol. **2:**401–409. http://dx.doi.org/10.1038/nri819.
13. **Liu FT, Newland AC, Jia L.** 2003. Bax conformational change is a crucial step for PUMA-mediated apoptosis in human leukemia. Biochem. Biophys. Res. Commun. **310:**956–962. http://dx.doi.org/10.1016/j.bbrc.2003.09.109.
14. **Sen N, Das BB, Ganguly A, Mukherjee T, Tripathi G, Bandyopadhyay S, Rakshit S, Sen T, Majumder HK.** 2004. Camptothecin induced mitochondrial dysfunction leading to programmed cell death in unicellular hemoflagellate *Leishmania donovani*. Cell Death Differ. **11:**924–936. http://dx.doi.org/10.1038/sj.cdd.4401435.
15. **Steele JC, Warhurst DC, Kirby GC, Simmonds MS.** 1999. *In vitro* and *in vivo* evaluation of betulinic acid as an antimalarial. Phytother. Res. 13:115–119. http://dx.doi.org/10.1002/(SICI)1099-1573(199903)13:2<115::AID-PTR404>3.0.CO;2-1.
16. **Reutrakul V, Anantachoke N, Pohmakotr M, Jaipetch T, Yoosook C, Kasisit J, Napaswa C, Panthong A, Santisuk T, Prabpai S, Kongsaeree P, Tuchinda P.** 2010. Anti-HIV-1 and anti-inflammatory lupanes from the leaves, twigs, and resin of *Garcinia hanburyi*. Planta Med. **76:**368–371. http://dx.doi.org/10.1055/s-0029-1186193.
17. **Laszczyk MN.** 2009. Pentacyclic triterpenes of the lupane, oleanane and ursane group as tools in cancer therapy. Planta Med. **75:**1549–1560. http://dx.doi.org/10.1055/s-0029-1186102.
18. **Chowdhury S, Mukherjee T, Sengupta S, Chowdhury SR, Mukhopadhyay S, Majumder HK.** 2011. Novel betulin derivatives as antileishmanial agents with mode of action targeting type IB DNA topoisomerase. Mol. Pharmacol. **80:**694–703. http://dx.doi.org/10.1124/mol.111.072785.
19. **Ramasamy S, Abdul Wahab N, Zainal Abidin N, Manickam S, Zakaria Z.** 2012. Growth inhibition of human gynecologic and colon cancer cells by *Phyllanthus watsonii* through apoptosis induction. PLoS One **7:**e34793. http://dx.doi.org/10.1371/journal.pone.0034793.
20. **Mullauer FB, Kessler JH, Medema JP.** 2009. Betulin is a potent anti-tumor agent that is enhanced by cholesterol. PLoS One **4:**e1. http://dx.doi.org/10.1371/journal.pone.0005361.
21. **Alakurtti S, Bergström P, Sacerdoti-Sierra N, Jaffe CL, Yli-Kauhaluoma J.** 2010. Anti-leishmanial activity of betulin derivatives. J. Antibiot. **63:**123–126. http://dx.doi.org/10.1038/ja.2010.2.
22. **Alakurtti S, Heiska T, Kiriazis A, Sacerdoti-Sierra N, Jaffe CL, Yli-Kauhaluoma J.** 2010. Synthesis and anti-leishmanial activity of heterocyclic betulin derivatives. Bioorg. Med. Chem. **18:**1573–1582. http://dx.doi.org/10.1016/j.bmc.2010.01.003.
23. **Domínguez-Carmona DB, Escalante-Erosa F, García-Sosa K, Ruiz-Pinell G, Gutierrez-Yapu D, Chan-Bacab MJ, Giménez-Turba A, Peña-Rodríguez LM.** 2010. Antiprotozoal activity of betulinic acid derivatives. Phytomedicine **17:**379–382. http://dx.doi.org/10.1016/j.phymed.2009.08.002.
24. **Mittra B, Saha A, Chowdhury AR, Pal C, Mandal S, Mukhopadhyay S, Bandyopadhyay S, Majumder HK.** 2000. Luteolin, an abundant dietary component is a potent anti-leishmanial agent that acts by inducing topoisomerase II-mediated kinetoplast DNA cleavage leading to apoptosis. Mol. Med. **6:**527–541. http://dx.doi.org/10.1007/s0089400060527.
25. **BoseDasgupta S, Das BB, Sengupta S, Ganguly A, Roy A, Dey S, Tripathi G, Dinda B, Majumder HK.** 2008. The caspase-independent

algorithm of programmed cell death in *Leishmania* induced by baicalein: the role of LdEndoG, LdFEN-1 and LdTatD as a DNA 'degradesome.' Cell Death Differ. **15:**1629–1640. http://dx.doi.org/10.1038/cdd.2008.85.
26. **McGuire SO, James-Kracke MR, Sun GY, Fritsche KL.** 1997. An esterification protocol for *cis*-parinaric acid-determined lipid peroxidation in immune cells. Lipids **32:**219–226. http://dx.doi.org/10.1007/s11745-997-0028-x.
27. **Mukherjee SB, Das M, Sudhandiran G, Shaha C.** 2002. Increase in cytosolic Ca^{2+} levels through the activation of non-selective cation channels induced by oxidative stress causes mitochondrial depolarization leading to apoptosis-like death in *Leishmania donovani* promastigotes. J. Biol. Chem. **277:**24717–24727. http://dx.doi.org/10.1074/jbc.M201961200.
28. **Boonstra J, Post JA.** 2004. Molecular events associated with reactive oxygen species and cell cycle progression in mammalian cells. Gene **337:**1–13. http://dx.doi.org/10.1016/j.gene.2004.04.032.
29. **Mattiazzi M, Vijayvergiya C, Gajewski CD, DeVivo DC, Lenaz G, Wiedmann M, Manfredi G.** 2004. The mtDNA T8993G (NARP) mutation results in an impairment of oxidative phosphorylation that can be improved by antioxidants. Hum. Mol. Genet. **13:**869–879. http://dx.doi.org/10.1093/hmg/ddh103.
30. **Jana NR, Dikshit P, Goswami A, Nukina N.** 2004. Inhibition of proteasomal function by curcumin induces apoptosis through mitochondrial pathway. J. Biol. Chem. **279:**11680–11685. http://dx.doi.org/10.1074/jbc.M310369200.
31. **Duchen MR.** 2000. Mitochondria and calcium: from cell signalling to cell death. J. Physiol. **529:**57–68. http://dx.doi.org/10.1111/j.1469-7793.2000.00057.x.
32. **Compton MM.** 1992. A biochemical hallmark of apoptosis: internucleosomal degradation of the genome. Cancer Metastasis Rev. **11:**105–119. http://dx.doi.org/10.1007/BF00048058.
33. **Tewari M, Quan LT, O'Rourke K, Desnoyers S, Zeng Z, Beidler DR, Poirier GG, Salvesen GS, Dixit VM.** 1995. Yama/CPP32 beta, a mammalian homolog of CED-3, is a CrmA-inhibitable protease that cleaves the death substrate poly (ADP-ribose) polymerase. Cell **81:**801–809. http://dx.doi.org/10.1016/0092-8674(95)90541-3.
34. **Ameisen JC.** 2002. On the origin, evolution, and nature of programmed cell death: a timeline of four billion years. Cell Death Differ. **9:**367–393. http://dx.doi.org/10.1038/sj.cdd.4400950.
35. **Ambit A, Fasel N, Coombs GH, Mottram JC.** 2008. An essential role for the *Leishmania major* metacaspase in cell cycle progression. Cell Death Differ. **15:**113–122. http://dx.doi.org/10.1038/sj.cdd.4402232.
36. **Gannavaram S, Vedvyas C, Debrabant A.** 2008. Conservation of the pro-apoptotic nuclease activity of endonuclease G in unicellular trypanosomatid parasites. J. Cell Sci. **121:**99–109. http://dx.doi.org/10.1242/jcs.014050.
37. **González IJ, Desponds C, Schaff C, Mottram JC, Fasel N.** 2007. *Leishmania major* metacaspase can replace yeast metacaspase in programmed cell death and has arginine-specific cysteine peptidase activity. Int. J. Parasitol. **37:**161–172. http://dx.doi.org/10.1016/j.ijpara.2006.10.004.
38. **Bodley AL, Shapiro TA.** 1995. Molecular and cytotoxic effects of camptothecin, a topoisomerase I inhibitor, on trypanosomes and *Leishmania*. Proc. Natl. Acad. Sci. U. S. A. **92:**3726–3730. http://dx.doi.org/10.1073/pnas.92.9.3726.
39. **Ganguly A, Das B, Roy A, Sen N, Dasgupta SB, Mukhopadhayay S, Majumder HK.** 2007. Betulinic acid, a catalytic inhibitor of topoisomerase I, inhibits reactive oxygen species-mediated apoptotic topoisomerase I-DNA cleavable complex formation in prostate cancer cells but does not affect the process of cell death. Cancer Res. **67:**11848–11858. http://dx.doi.org/10.1158/0008-5472.CAN-07-1615.
40. **Sharma RK, Garg BS, Kurosaki H, Goto M, Otsuka M, Yamamoto T, Inoue J.** 2000. Aurine tricarboxylic acid, a potent metal-chelating inhibitor of NFkappaB-DNA binding. Bioorg. Med. Chem. **8:**1819–1823. http://dx.doi.org/10.1016/S0968-0896(00)00109-7.
41. **Hill MM, Adrain C, Duriez PJ, Creagh EM, Martin SJ.** 2004. Analysis of the composition, assembly kinetics and activity of native Apaf-1 apoptosomes. EMBO J. **23:**2134–2145. http://dx.doi.org/10.1038/sj.emboj.7600210.
42. **Lee N, Gannavaram S, Selvapandiyan A, Debrabant A.** 2007. Characterization of metacaspases with trypsin-like activity and their putative role in programmed cell death in the protozoan parasite *Leishmania*. Eukaryot. Cell **6:**1745–1757. http://dx.doi.org/10.1128/EC.00123-07.